This is to certify that the
thesis entitled

ANALYSIS OF ALKALI METAL-CATIONIZED
PHARMACEUTICALS USING ELECTROSPRAY IONIZATION
TANDEM MASS SPECTROMETRY

presented by

SUSAN LYNN ACHBERGER

has been accepted towards fulfillment
of the requirements for the

Master of Science	degree in	Biochemistry and Molecular Biology

A. Daniel Jones
Major Professor's Signature

8/19/2008
Date

ANALYSIS OF ALKALI METAL-CATIONIZED PHARMACEUTICALS USING ELECTROSPRAY IONIZATION TANDEM MASS SPECTROMETRY

By

Susan Lynn Achberger

A THESIS

Submitted to
Michigan State Univeristy
in partial fulfillment of the requirements
for the degree of

MASTER OF SCIENCE

Department of Biochemistry and Molecular Biology

2008

ANALYSIS OF ALKALI METAL-CATIONIZED PHARMACEUTICALS USING ELECTROSPRAY IONIZATION TANDEM MASS SPECTROMETRY

By

Susan Lynn Achberger

The effect of alkali metal cations (Li^+, Na^+, and K^+) on the collision-induced dissociation of the pharmaceuticals ciprofloxacin, levofloxacin, and erythromycin was investigated using electrospray ionization tandem mass spectrometry (ESI-MS/MS). For both levofloxacin and erythromycin, alkali metal cationization yields molecular fragments that were not obtained using protonation. In the case of erythromycin, lithium and sodium cationization yields fragmentation of the macrolide ring, thus providing information about this particular structural feature of the molecule, which was not obtained for protonated samples. Data also indicate that the varying ion mobility of H^+, Li^+, Na^+, and K^+ yields different fragmentation pathways. These experiments demonstrate that alkali metal cationization can provide a method for the structural determination of pharmaceuticals and their metabolites.

DEDICATION

To my parents Bill and Jan Achberger
and my furry friend Skip Achberger,
for your unconditional love and support

And to my undergraduate advisor,
Dr. Norman J. Wells
(May 5, 1948 – January 7, 2006),
for everything you did for me

ACKNOWLEDGMENTS

To my advisor, Dr. A. Daniel Jones: Thank you for helping/putting up with a stubborn, misguided graduate student. You taught me so much and I cannot thank you enough for your patience and compassion.

To Dr. Ruth Waddell-Smith: Thank you for serving on my committee and for your willingness to provide a listening ear. Most importantly, thank you for being a mentor and a friend. You were with me from the very beginning and I could not have done any of this without you.

To Dr. Robert Hausinger: I have greatly enjoyed working with you as a committee member and professor. Your time and input are very much appreciated.

To the members of the Jones Laboratory, especially Siobhan Shay, Michael Stagliano, and Ruth Udey: I am so fortunate to have such wonderful coworkers who are equally wonderful friends. Thank you for all of your help and support. Please accept a delicious bass as a sign of my gratitude.

To my fellow MSU graduate students, Julie Bordowitz, David and Heather Dotzauer, Kate Higginbotham, Aaron McBride, Eric Moellering, Danielle Nevarez, and Aggie Steiner: I am so thankful that I have wonderful friends who shared this crazy journey with me. Thank you for your friendship, encouragement, and unfaltering support.

To my friends, Kimberly Moherman, Jessica Davila, Anita Dasu, Laura Johns-Fowler, Stephanie Schuster-Maglis, and Alexis Witt: Even though we were miles apart throughout my graduate school experience, I never felt far from you. I appreciate your friendship, guidance, and "pep talks," and I cannot express how grateful I am for all you have done for me.

To the congregation of the Okemos Community Church, especially the members of the handbell and chancel choirs: Thank you for all of your prayers and support. You were my family during my time at MSU and I am very blessed to have you in my life. You also served as a constant reminder that I am loved and I could not have done this without your love and support. Words cannot express my gratitude.

Table of Contents

List of Figures

Chapter 1

Chapter 2

Appendix I

List of Tables

Appendix II

Key to Abbreviations

CID	Collision-induced dissociation
CYP	Cytochrome P450 (metabolic enzymes)
ESI	Electrospray ionization
FIA	Flow-injection analysis
GC	Gas chromatography
H/D	Hydrogen-deuterium exchange
LC	Liquid chromatography
Met^+	Alkali metal cation
MS	Mass spectrometry
MS/MS	Tandem mass spectrometry

CHAPTER 1: INTRODUCTION AND BACKGROUND

Background

Metabolomics, the term given to assessing the entire array of metabolites, provides a powerful tool for the potential treatment and diagnosis of diseases and the discovery and development of new pharmaceuticals. In the pharmaceutical industry, comparing the metabolome of an organism with and without the presence of a drug is critical for the discovery of new pharmaceuticals. This will allow for the elucidation of the structure of the drug's metabolites, as well as the determination of the effect of the drug on biological pathways. Because many enzymes are capable of metabolizing more than one compound, this can lead to drug-drug interactions, during which one drug interferes with the metabolism of another, leading to adverse effects. As a result, the requirement for analytical techniques that can analyze metabolites in order to determine their molecular structure has greatly increased. In this project, mass spectrometry, a valuable technique for the characterization of metabolites, will be used to provide information regarding the molecular structures of various pharmaceutical substrates, with the aim of developing tools useful for elucidation metabolite structures.

One of the greatest challenges involved in metabolite analysis and metabolic technology development is the distinction between isomeric and isobaric metabolites. Oxidation is one of the most common metabolic transformations, and many compounds can undergo metabolic oxidation at multiple sites. For example, 5-hydroxyomeprazole and omeprazole sulfone are the main metabolites in human *in vitro* metabolism of omeprazole, catalyzed by the cytochrome (CYP) 450 enzymes CYP3A4 and CYP2C19

respectively. Both of these metabolic alterations cause a mass shift of +16 units, making distinguishing these two structures challenging [1, 2]. Also, because various isomers can have different toxicological properties, structural information about these compounds can provide information about the potential toxicity of a compound. For example, the drug thalidomide was administered as a racemic mixture to pregnant women in the 1960s to prevent morning sickness. Thalidomide was later determined to be teratogenic and this toxic effect was eventually attributed to one of thalidomide's hydroxylated metabolites, though the exact metabolite was not specified [3, 4].

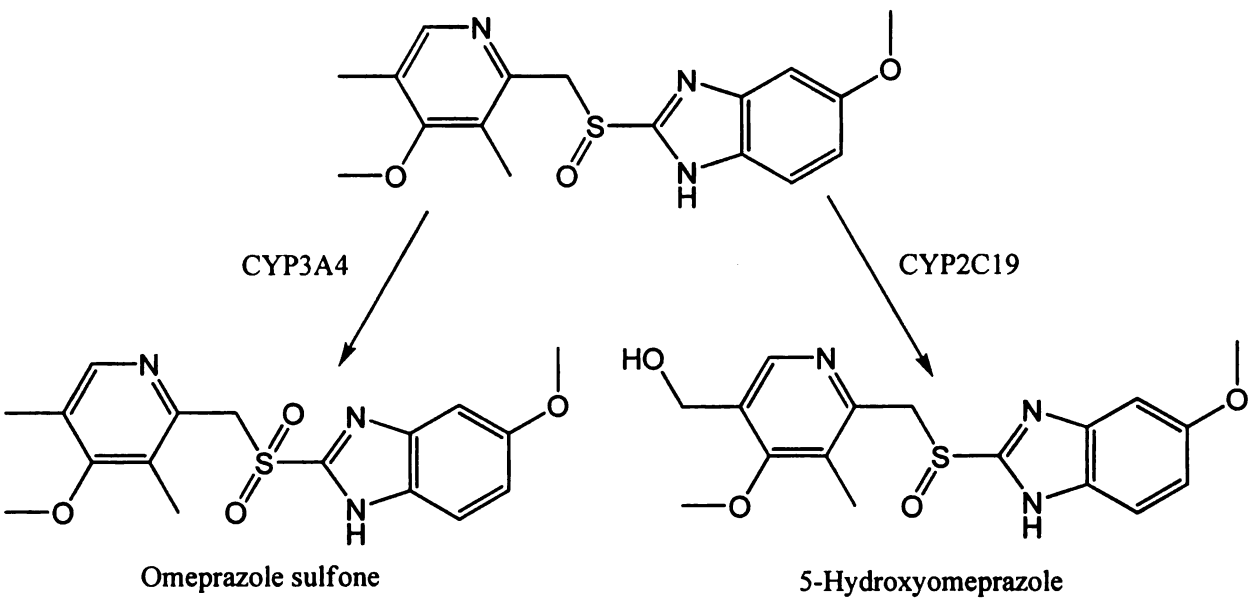

Figure 1. Structures of omeprazole and two isomers of its oxidative metabolites [1, 2]

Drug metabolism can also lead to adverse drug-drug interactions. CYP 450 enzymes are considered the most important first step in metabolism of most drugs and humans express 18 families and 43 subfamilies of CYPs. CYP families 1, 2, and 3 are responsible for xenobiotic metabolism and are the determinants of elimination and bioavailability of pharmaceutical compounds. Specifically, CYPs 1A2, 3A4, 2D6, 2C9,

and 2C19 metabolize over 90% of human drugs [5]. CYP-dependent metabolism can increase the efficacy of a drug (bioactivation), promote elimination of the metabolite from the body by forming more polar metabolites, or can generate electrophilic metabolites that exhibit toxicity. Drugs and other environmental and endogenous substances can lead to the inhibition or induction of CYP enzymes, which influences drug-drug interactions in patients undergoing multi-drug therapy [5].

One example of this phenomenon is the adverse interactions between haloperidol, an antipsychotic drug, and valerian, an herbal sleep aid. The findings of Dalla Corte et al. [6] indicate that adverse drug-drug interactions take place between valerian and haloperidol, leading to oxidative stress in the liver. They propose that valerian and other herbal supplements can change the metabolism of haloperidol through the inhibition or induction of CYP450 enzymes. CYP3A4 and 2D6 have inductive effects on valerian *in vitro*, and such alterations can affect the disposition of other drugs that are taken concurrently [7].

Umathe et al. [8] observed a similar phenomenon with the compounds quercetin and pioglitazone. Quercetin, often contained in herbal add-on therapy for diabetes, inhibits CYP3A4, which is responsible for metabolizing the antidiabetic drug pioglitazone. Since quercetin inhibits CYP3A4's ability to metabolize pioglitazone, the bioavailability of pioglitazone increases, thus lowering the rate of hepatic clearance.

CYP3A4 is involved in the metabolism of 60% of all therapeutically used drugs and its levels in the human liver can be increased or decreased because of a patient's exposure to numerous drugs [6, 10]. This can create a problem during the pharmaceutical development process. If the same enzyme is responsible for the metabolism of many

drugs, this can lower the efficacy of the respective drugs because they are all competing to interact with that particular enzyme. Determination of CYP-mediated metabolism of new candidate drugs, including identification of specific sites of enzyme-catalyzed metabolism, is necessary during the development of pharmaceutical compounds to ensure the safety and efficacy of those compounds. As a result, improved methods for metabolite structure elucidation are needed in order to determine the metabolic pathways responsible for biotransformation of that compound, and to determine whether toxic metabolites are generated.

Introduction to Mass Spectrometry

Mass spectrometry (MS) is the dominant analytical technique that is used to determine the molecular weights of chemical compounds during the drug development process. This technique can also be used to help elucidate the structures of drugs and their metabolites. In mass spectrometry, ions are separated based upon their mass-to-charge ratio (m/z). These ions are created through acquisition of a charge, such as protonation or cationization, by neutral molecules [9]. Figure 2 presents a schematic of the mass spectrometry process.

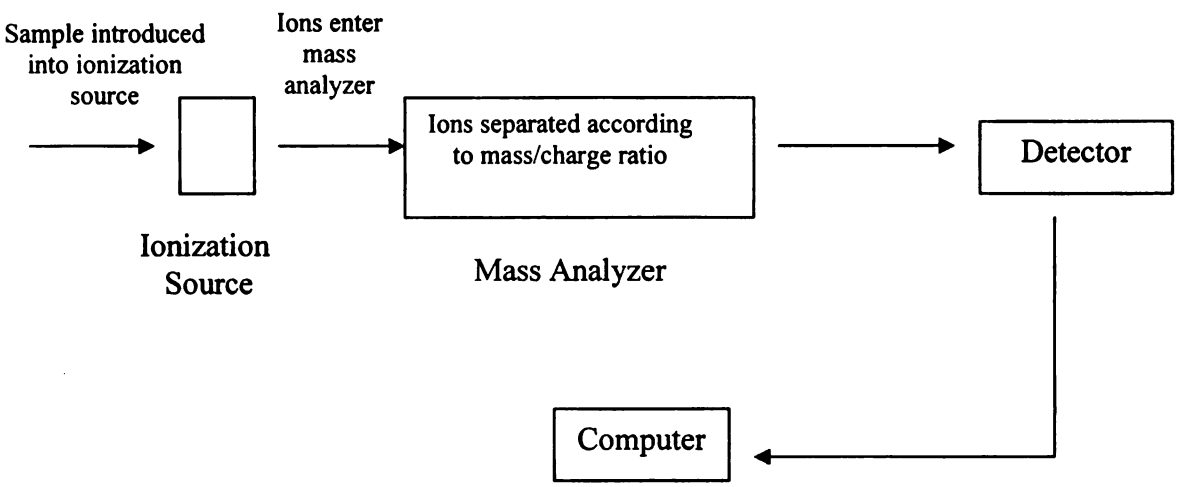

Figure 2. Schematic of the mass spectrometry process

Upon introduction into the instrument, analyte molecules undergo ionization in the ion source. The resulting ions are propelled by electric fields into the mass analyzer and then separated based upon their mass-to-charge ratios through various combinations of electric and magnetic fields. The detector enables the mass spectrometer to amplify an electrical signal from the incident ions, convert the ion current to voltage, and convert the

analog voltage to a digital measure of ion abundance. That digital measure of ion signal is then transferred to a computer that can be used for data processing [9].

Electrospray Ionization (ESI)

Electrospray ionization (ESI), an ionization technique used to generate gas-phase ionized molecules from a liquid solution, has emerged during the past few years as an essential tool for the analysis of proteins, polymers, and small polar molecules. It allows for detection of femtomole quantities and is easy to couple to liquid chromatography (LC) [10]. Figure 3 presents a schematic of an ESI source.

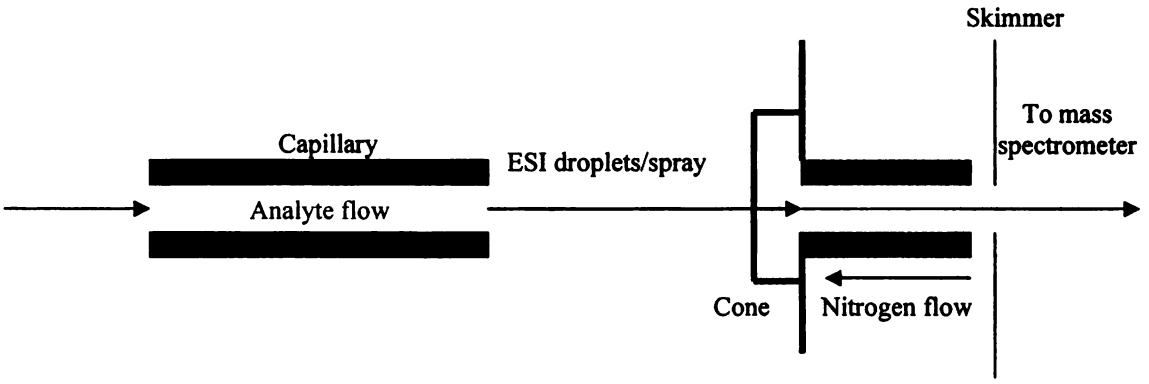

Figure 3. Schematic of an ESI source [11, 12]

To generate these ionized molecules, a fine spray of highly charged droplets is created in the presence of a strong electric field. In ESI, which occurs at atmospheric pressure, a strong electric field is applied to a liquid passing through a capillary tube. Figure 3 illustrates the mechanism of ESI, which is described below.

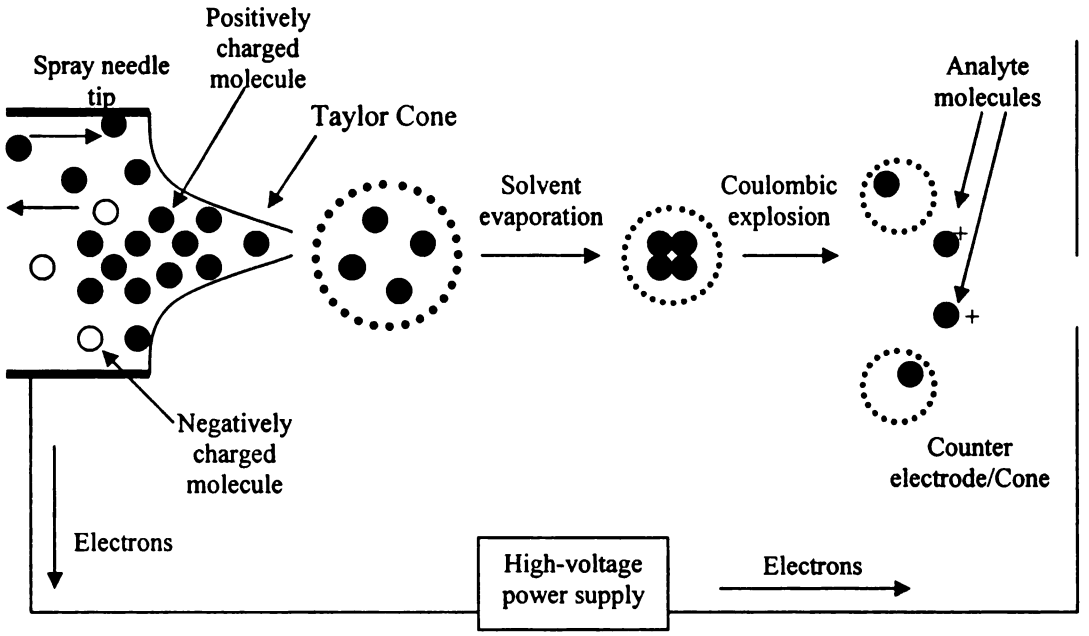

Figure 4. A schematic of the ESI mechanism, shown in positive ionization mode [11, 12]

The electric field causes charge accumulation at the surface of the liquid that is emerging from the end of the capillary tube. The excess charge in the liquid solution distorts the liquid shape to form a Taylor cone, and electrostatic repulsion drives the liquid to break apart to form highly charged droplets. Then, the droplets travel through a heated capillary or a curtain of inert gas, typically nitrogen, where collisions cause evaporation of solvent molecules. The droplets shrink and their charge per unit volume increases as the solvent evaporates. Ions are then generated as the charged molecules are desorbed from the droplet's surface [12, 15].

ESI typically yields ions via deprotonation (negative ions), or via protonation, or cationization to form positive ions. In the case of protonation, a proton will be added to a molecule to yield a net positive charge of 1+ for each proton that is added. For example,

large analyte molecules, such as proteins, can have multiple charges if multiple ionizable sites are present.

ESI is considered a "soft" ionization technique because intact molecular ions can be produced with minimal fragmentation [13]. This stands in contrast to traditional electron ionization which usually generates many ions consisting of fragments of the original molecule. Because ESI occurs at atmospheric pressure, minimal energy is transferred to the analyte during ionization, and little or no fragmentation occurs in the ion source. As a result, mass spectra of most compounds show only protonated or cationized ions in positive ion mode. While this is useful for molecular weight determination, these mass spectra lack fragment ions that give information regarding structure.

Tandem Mass Spectrometry (MS/MS) and Collision-Induced Dissociation (CID)

More structural information can be obtained using tandem mass spectrometry (MS/MS), which involves the activation of a particular precursor ion, generation of fragment ions, and the mass analysis of the fragmentation products. Tandem mass spectrometry refers to any method that involves two stages of mass analysis that are combined with either a dissociation process or a chemical reaction that can alter the charge or mass of an ion. Figure 5 is a schematic of the tandem mass spectrometry process.

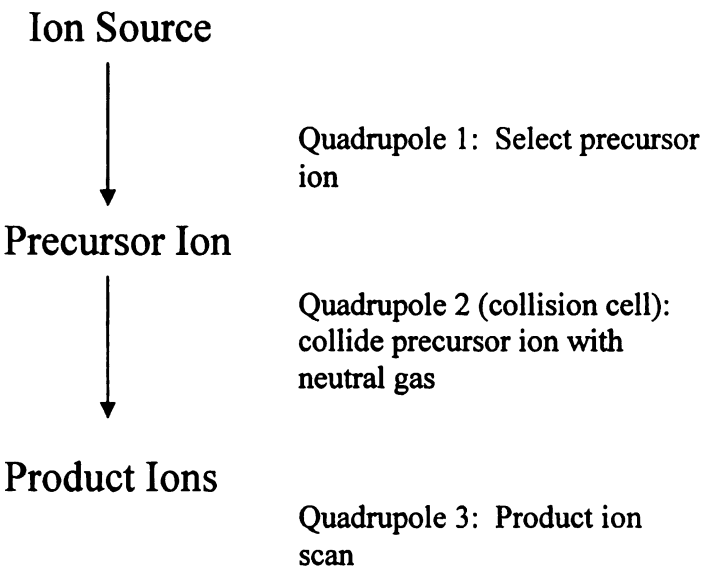

Figure 5. Schematic of the tandem mass spectrometry process

In one kind of MS/MS experiment, referred to as tandem mass spectrometry in space, the first mass analyzer isolates a precursor ion of a specific m/z that will subsequently undergo fragmentation to give product ions and neutral fragments. A second mass analyzer is used to analyze the masses of the product ions. The number of steps in tandem mass spectrometry can also be increased. For example, a user can select ions of a first particular mass, then select ions of a second particular mass from the fragments that were obtained, and analyze the fragments of the last selected ions. The quantity of these steps can be augmented to give MS^n experiments, where n is the number of generations of ions being analyzed [10].

One way to conduct MS/MS experiments is to couple two physically distinct instruments. This technique is known as tandem mass spectrometry in space. Tandem in space instruments include two mass analyzers. Frequently, a type of analyzer called a quadrupole is used in these types of instruments. The triple quadrupole, or QqQ

configuration, is an instrument that consists of three quadrupoles. This configuration was developed at Michigan State University by Chris Enke and Richard Yost in the 1970s [14]. The first quadrupole is used to select the precursor ions, the second quadrupole, q, is the collision cell that performs no mass filtering, and the third quadrupole analyzes the product ions [10]. This is shown in Figure 5. In the collision cell, ions selected by quadrupole 1 are activated by collisions with neutral gas molecules. This technique is known as collision-induced dissociation (CID), which is illustrated in Figure 6.

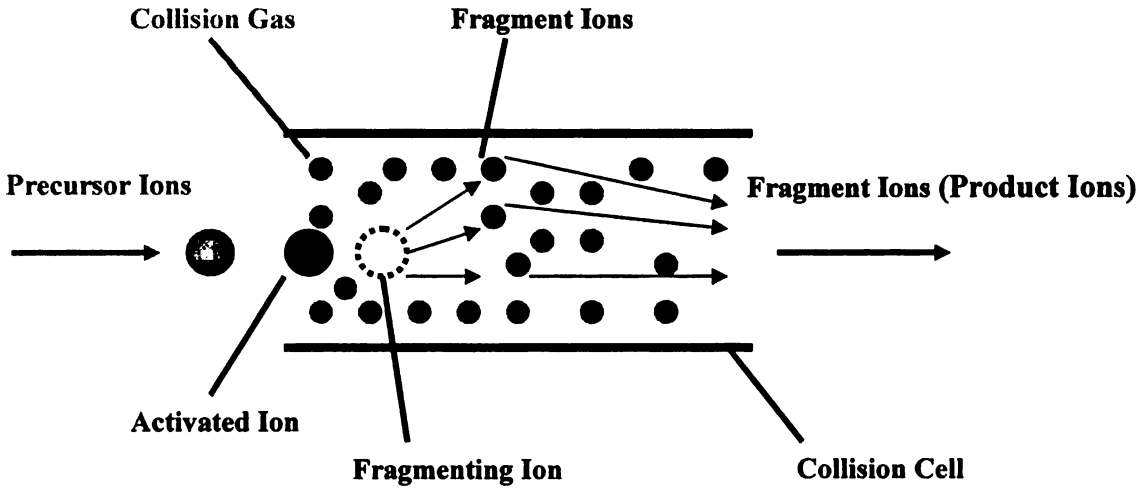

Figure 6. Schematic of the collision-induced dissociation (CID) process

When the precursor ion collides with a neutral target gas, the kinetic energy of the precursor ion is converted into internal energy, causing subsequent fragmentation [15]. The ion will fragment when the internal energy has accumulated in the appropriate vibrational modes of the bonds in the molecule to allow fragmentation reactions to occur on the time scale of the ion's transit through the collision cell.

Fragmentation of an activated ion can occur through multiple reaction pathways. Figure 7 shows an example of two possible fragmentation pathways that can occur for the CID of the ionized molecule A-B.

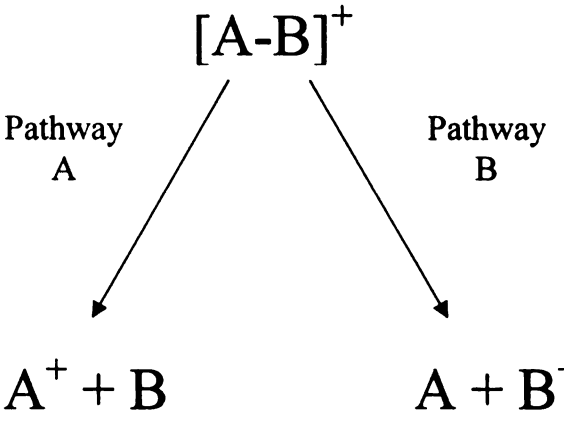

Figure 7. The possible fragmentation pathways for molecule $[A\text{-}B]^+$

The fragmentation observed in a mass spectrum is dictated by the amount of internal vibrational energy in the precursor ion and the activation energy barrier that must be overcome in order to produce the observed fragments. For example, if the activation energy barrier for Pathway A is lower than that of Pathway B, and if the internal energy is too low to yield an appreciable rate of reaction for Pathway B, the fragmentation reaction that generates the A^+ ion will occur more rapidly than through Pathway B, and only the A^+ ion will be observed as a fragment. Portion B of the molecule, which is lost as a neutral species, will not be observed in the mass spectra. Increasing the internal energy may provide enough energy for reaction through Pathway B to occur, but the lower activation barrier to Pathway A may result in its product dominating the spectrum regardless of experimental conditions. In such situations, if molecule A-B was a metabolite, any structural features present on portion B would not be observed in the

form of fragment ions. In order to observe the B^+ ion in the mass spectra, the activation energy needed to enable the molecule to dissociate via Pathway A needs to be raised to allow Pathway B to become competitive. A method to control and enhance the fragmentation pathways of a molecule is needed in order to identify any metabolic structural modifications that have occurred, and to determine the position of those modifications.

Cationization

Metal cationization, when used with ESI mass spectrometry (ESI-MS), is an ionization mechanism that can provide enhanced molecular structure information that often cannot be obtained utilizing traditional protonation. A charged complex is formed during the cationization process, in which a positively charged ion such as an alkali metal ion forms a complex with a neutral molecule [9]. When using ESI, metal ion adducts of organic molecules are observed. Analytes that lack basic functional groups are often difficult to protonate, whereas they readily form complexes with alkali metal ions. Metal cationization is easy to perform, requiring only the addition of a salt to the electrosprayed solution. Only a small amount (pmoles or less) of the sample is needed. Metal cationized ions may fragment through different pathways compared to protonated ions [16]. Attachment of alkali metal cations can localize charge on different sites on the molecule than would be the case for proton attachment, owing to different affinities of functional groups for protons compared to metal cations. Some fragmentation reactions are driven by proximity to charge whereas others occur remote from charge attachment.

Altering the balance between pathways and encouraging charge-remote fragmentation has been used to determine the structure of lipids [17, 18].

Charge-remote fragmentation occurs when gas-phase decompositions, like those observed in CID, take place at a location that is physically remote from the charge site on the molecule. Protonated molecules often fragment largely via charge-directed fragmentation. The proximity of a positive charge can draw electron density from nearby bonds, weakening them and encouraging fragmentation. Since protons are mobile owing to their low mass and high velocities and vibrational frequencies, proton migration can induce fragmentation to occur at multiple locations in an ion [10, 19]. Because alkali metal cations have much greater masses than a proton, their velocities are lower at the same vibrational energies and they are less able to migrate across molecules to facilitate multiple fragmentation reactions. For example, Lopes and coworkers conducted fragmentation studies on the antibiotic monensin A, and determined that protonated and sodium-cationized samples have different fragmentation pathways [20-22]. This method has also been used in CID experiments involving sugars [23] and fatty acids [24-27]. For example, lithium cationization, coupled with CID, had been used to determine the type of carbohydrate linkage, such as a $\beta 1 \rightarrow 4$ linkage between two glucose molecules [28], as well as the location of double bonds in fatty acids, esters, and alcohols [29, 30].

Dörr et al. [31] used ESI-MS^n to investigate the effect of differential ion mobility of H^+, Li^+, Na^+, and K^+ on the fragmentation pathways of cylindrospermopsin, a zwitterionic toxin produced by cyanobacteria (Figure 8).

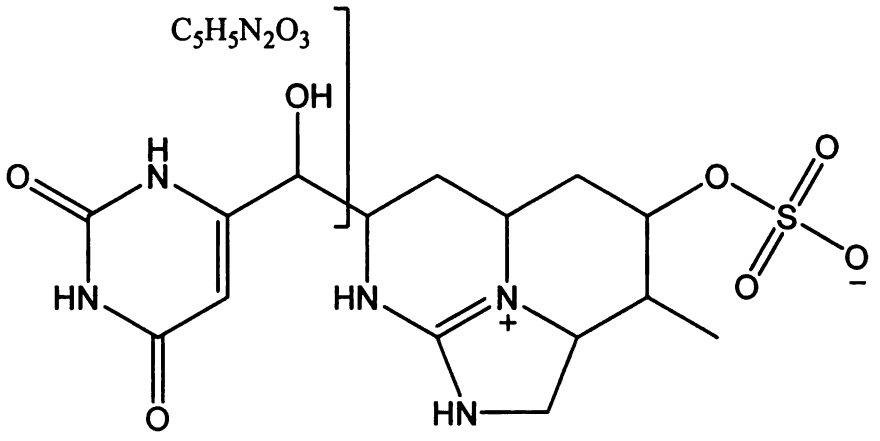

Figure 8. Structure of cylindrospermopsin

Upon comparison of protonated and cationized spectra, they observed a difference in the balance of terminal ring elimination between the two species (this pathway becomes more prominent as the mass of the cation increases) when ion intensity ratios for appropriate fragment ions were compared. Also, the lithiated spectra showed more diverse fragmentation than sodium-cationized species, but no proposed structures or mechanisms were shown for the lithiated cylindrospermopsin. Potassium cationization yielded unique spectra as well, but again, no proposed structures or mechanisms were discussed for potassium-cationized species. As Dörr et al. discuss, their proposed fragmentation pathway 1, which involves a loss of $C_5H_6N_2O_3$, becomes more prominent as the atomic mass of the charged species increases. As a result, Dörr et al. determined that the higher atomic mass of the migrating cations can alter the fragmentation pathways observed in CID spectra, but their work failed to provide detailed explanations for these differences.

Cui et al.[16] also used ESI-MS^n to investigate the effect of metal (Li^+, Na^+, K^+, Ag^+) cationization on the CID of ginsenosides, the compounds that give ginseng its

pharmaceutical properties. The general structure of a ginsenoside is shown in Figure 9, where the respective R groups can be various sugars or hydroxyl groups.

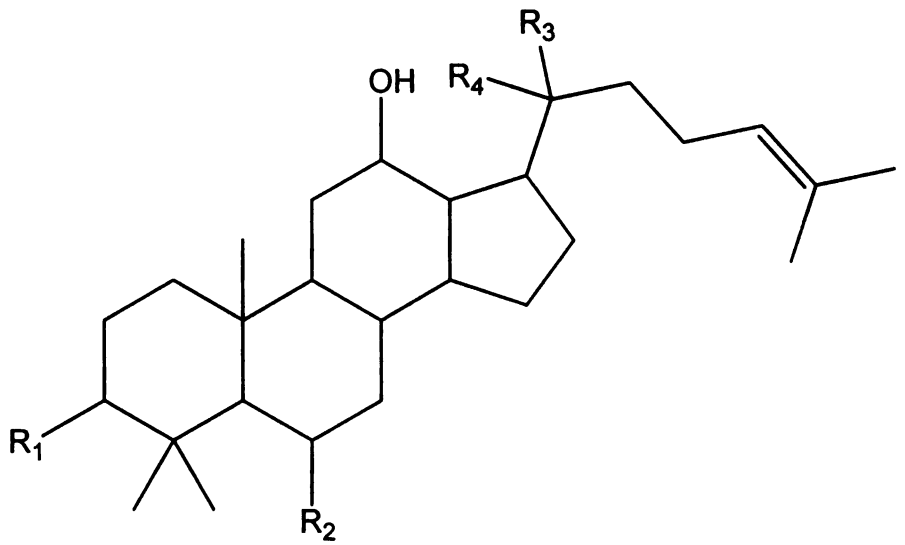

Figure 9. The backbone structure of a ginsenoside with R groups corresponding to hydroxyl or sugar groups

They determined that the species of metal ion and the structure of the ginsenoside affect the interaction between the ginsenoside and the metal ion. Specifically, the number of oxygen atoms present in each ginsenoside affects the metal ion coordination. For example, they observed that lithium-cationization yields a greater array of fragment ions when compared to the other metal-cationized species. This indicates that, because if its small mass, lithium can move around the surface of the molecule and cause bond cleavage at different locations in the molecule, yielding a wider range of charge-directed dissociation reactions than sodiated species. They also observed that sodium-cationized species have lower fragmentation efficiencies than lithium-cationized species. Since sodium has a greater atomic mass than lithium, its velocity is lower, and it is less likely to migrate across the molecule to the same extent as lithium. As a result, fewer fragmentation reactions are observed with sodium cationization. Fewer fragmentation

reactions were observed for potassium-cationized species for the same reason. Also, Cui and coworkers determined that, as the size of the metal ion increases, the number of oxygen atoms in the ginsenoside that are able to coordinate to the metal ion increases, which fixes the charge in fewer locations and leads to more prominence for charge-remote dissociation.

The work conducted by Cui et al. and Dörr et al. demonstrates that cationization can yield different fragmentation pathways than those observed with protonation. Applying this concept to the example in Figure 7, cationization could be used to raise the barrier to Pathway A and direct ion $A\text{-}B^+$ to fragment via Pathway B. Because different cations can guide fragmentation to occur through different pathways for the same molecule, this technique can be applied to the MS analysis of pharmaceutical and biological compounds to aid structure determination. Cationization will provide a method to control the fragmentation of pharmaceutical compounds and thus determine the location of structural modifications that have occurred during metabolism.

CHAPTER 2: COLLISION-INDUCED DISSOCIATION MASS SPECTROMETRY OF METAL CATIONIZED XENOBIOTICS AND THEIR METABOLITES

Introduction

Mass spectrometry (MS) is the primary tool used for identification of xenobiotic compounds and their metabolites owing to the low detection limits afforded by this technique. The typical approach for MS-based structure characterization involves conversions of molecular ion species into fragment ions and determination of the fragment ion masses. The power of MS lies in its ability to provide critical information about molecular masses, and the presence of molecular substructures can be established based upon masses of fragment ions.

One of the primary limitations to the use of MS for structure elucidation involves limited control of the fragmentation process. Some ions are resistant to fragmentation owing to large activation barriers to formation of fragment ions. In contrast, other molecular ions undergo a single facile fragmentation that leads to formation of a dominant fragment ion that only conveys information about a single structural feature. Examples of this include losses of neutral water or carbohydrate groups, yielding fragments that present minimal information about molecular structure. To address these limitations, improved mass spectrometry methods are needed to enhance and control fragmentation. The most common ions generated during LC/MS analyses are protonated, or $[M+H]^+$ ions. Protonation of groups such as alcohols provides a low activation barrier, compared to other fragmentation pathways, to elimination of groups such as water. Formation of ions other than via protonation offers the possibility of increasing activation

barriers, and thus allowing a greater fraction of the ionized molecules to fragment via other reaction pathways.

In this study, protonated and alkali metal-cationized antibiotics ciprofloxacin, levofloxacin, and erythromycin were generated using electrospray ionization to determine whether metal cationization could be used to control the ion fragmentation dynamics. Ciprofloxacin and levofloxacin (Figure 10) belong to a class of antibiotic compounds known as fluoroquinolones which inhibit topoisomerases involved in bacterial DNA metabolism [32]. Some fluoroquinolones have caused serious toxic reactions, leading to their withdrawal from the market or restrictions on their use. Over a wide range of doses, ciprofloxacin and levofloxacin are two of the best-tolerated and safest fluoroquinolones [32]. Even though ciprofloxacin is one of the safest fluoroquinolones, when administered concurrently with the asthma medication theophylline, it can inhibit CYP 450 enzymes, thus blocking the metabolism of theophylline *in vitro* [33].

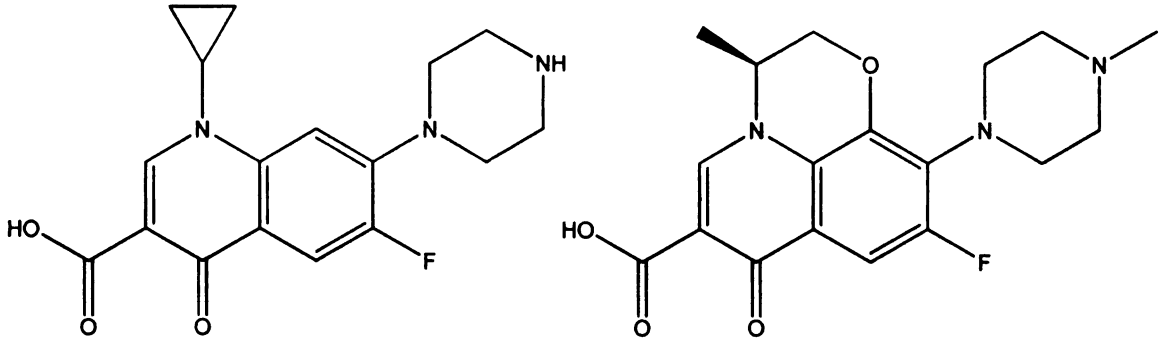

Figure 10. Chemical structures of the fluoroquinolone antibiotics ciprofloxacin (left) and levofloxacin (right)

Fragmentation of protonated and metal ion-cationized erythromycin (Figure 11), a macrolide polyketide antibiotic, was also investigated in this study. While erythromycin is an effective antimicrobial compound, it has also been shown to cause liver dysfunction

[34, 35]. For example, Karthek and Casson [35] reported a case of erythromycin-associated liver dysfunction in a ten-year-old girl. They state that erythromycin transient liver dysfunction is rarely reported in the pediatric literature, but it has been commonly reported in adults. While the exact mechanism of erythromycin-associated liver injury is unknown, one hypothesis is that a metabolite of erythromycin could cause an immunological response, thus resulting in liver injury.

Erythromycin and its analogs are metabolized by CYP450s, which can lead to the formation of stable metabolic intermediate complexes with CYP450s [36, 37]. These complexes are inactive and thus inhibit the metabolism of other drugs that are taken concurrently [37]. Also, metabolism of erythromycin by various CYP450 enzymes creates isomers because multiple cites of hydroxylation are possible. Different CYP450 isoenzymes may hydroxylate erythromycin at different positions. To establish which CYP450s might be involved in erythromycin metabolism, there is a need for analytical tools that can distinguish sites of hydroxylation.

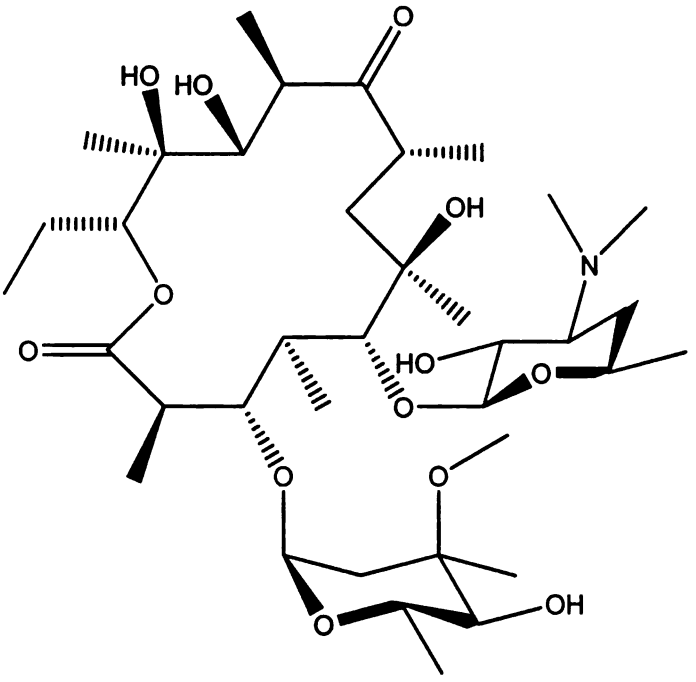

Figure 11. Chemical structure of the macrolide antibiotic erythromycin.

Development of a suitable technique for the structural characterization of xenobiotic metabolites is important as this could provide useful information about involvement of specific CYP450 isoenzymes with xenobiotic biotransformation, and could serve as indicators of likelihood that a xenobiotic could interfere with the metabolism of other endogenous or exogenous compounds

Collision-induced dissociation MS/MS spectra of the protonated and cationized forms of levofloxacin, ciprofloxacin, and erythromycin were compared in this study. Because alkali metal cations have a greater mass than a proton and will therefore migrate between functional groups more slowly, metal cationization increases energy barriers to migration of the attached cation throughout the analyte molecule and can direct fragmentation to occur via alternate reaction pathways. It is anticipated that

fragmentation directed to occur through different reactions will generate structurally useful fragment ions that would not form analogous ions for protonated molecules.

Methodology

FIA-ESI/MS/MS of Protonated and Cationized Pharmaceuticals

Standards of erythromycin, levofloxacin, ciprofloxacin, and all alkali salts were purchased from Sigma-Aldrich. Standards were prepared in MilliQ water/HPLC grade methanol (50:50, v:v) at a concentration of 10 μM. The water/methanol solution was also used as a blank. Cationized samples were prepared as above, with 10 μL of a 1 M solution of lithium acetate, sodium acetate, or potassium acetate added to each sample to give a metal salt concentration of 10 mM.

Samples were analyzed by flow-injection analysis (FIA) ESI-MS/MS. Injection volume was 20 μL ESI mass spectra and CID spectra were obtained using a Quattro Premier XE triple quadrupole mass spectrometer (Waters, Milford, MA). Samples were introduced into the electrospray source from an Acquity Ultra Performance LC (Waters) and analyzed in positive ion mode with a cone voltage of 30 V. Solvents used were 0.15% formic acid in water and acetonitrile (50:50) with a flow rate of 0.2 $mLmin^{-1}$ for erythromycin, and a flow rate of 0.1 $mLmin^{-1}$ for the fluoroquinolone samples. The $[M+H]^+$, $[M+Li]^+$, $[M+Na]^+$, or $[M+K]^+$ ion was selected as the parent ion for CID. For CID experiments, collision voltages of 10, 25, 40, and 55 V were used. Collision voltages of 10, 25, 30 and 35 V were used for lithiated and sodiated fluoroquinolone samples. Argon was used as the collision gas at a pressure of 2.73×10^{-3} mbar.

Pseudo-MS^3 experiments were conducted for lithium- and sodium-cationized samples of levofloxacin, ciprofloxacin, and erythromycin as above with a cone voltage of 95 V used for MS analysis. These experiments use in-source collisional activation to

generate fragment ions, and these fragment ions can be induced to fragment further in the instrument's collision cell. This information assists with assignments of fragmentation pathways that proceed through specific ion intermediates. Parent ions selected for CID were based upon proposed fragment structures illustrated in Figure 14, Figure 17, Figure 21, Figure 24, Figure 35, and Figure 41. These ions were selected to confirm the proposed fragmentation pathways.

Hydrogen-deuterium (H/D) exchange experiments were conducted to verify the proposed fragmentation mechanisms for protonated and cationized samples of each respective compound. These experiments indicate the number of exchangeable hydrogens present on the analyte molecule and its fragments, thus suggesting which hydrogen atoms are involved in migrations that lead to fragmentation. Samples were prepared as above with the use of 99-atom% deuterium oxide (Isotec, Inc.) instead of water. Samples were analyzed as described previously.

Results

Fluoroquinolones: Ciprofloxacin and Levofloxacin

Protonated Species

CID spectra for levofloxacin are shown in Figure 12 and Figure 13, and the proposed fragmentation pathways are depicted in Figure 14. Similarly, CID spectra for ciprofloxacin are shown in Figure 15 and Figure 16 and the proposed fragmentation pathways are depicted in Figure 17. CID spectra shown in the aforementioned figures serve as the primary data for the proposed pathways, and the rationale underlying these conclusions is described below.

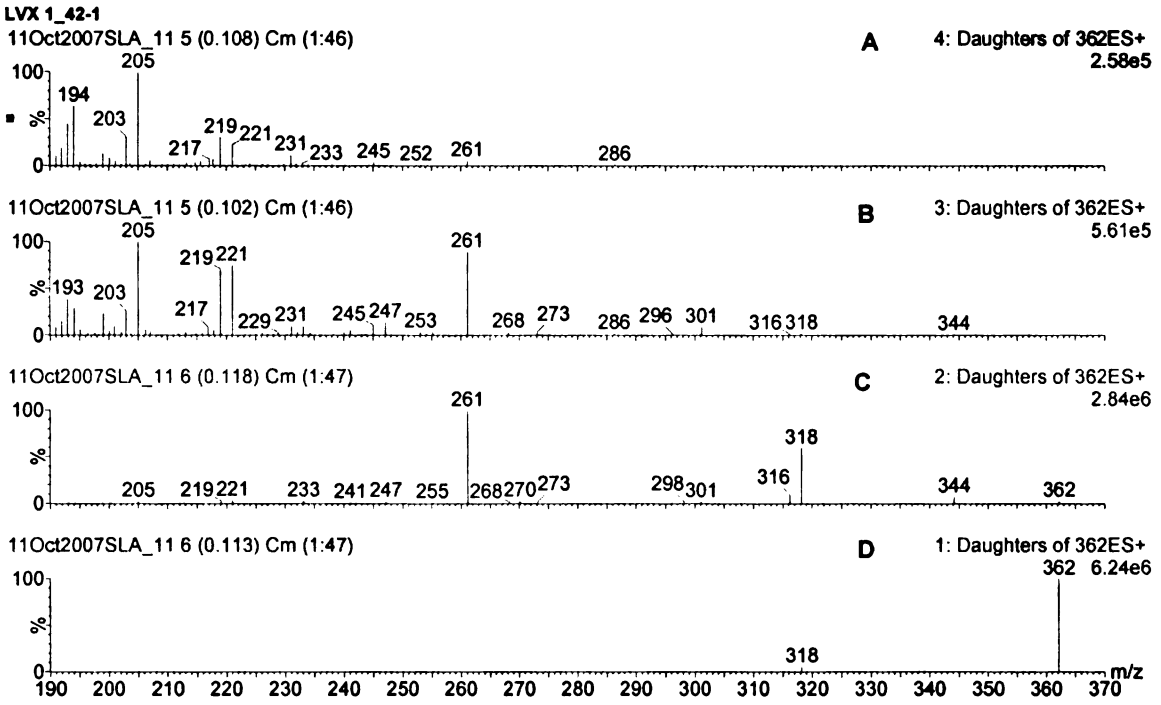

Figure 12. CID product ion spectra for protonated levofloxacin (m/z 362) at collision cell potentials of (A) 55 V, (B) 40 V, (C) 25 V, and (D) 10 V using argon as a collision gas

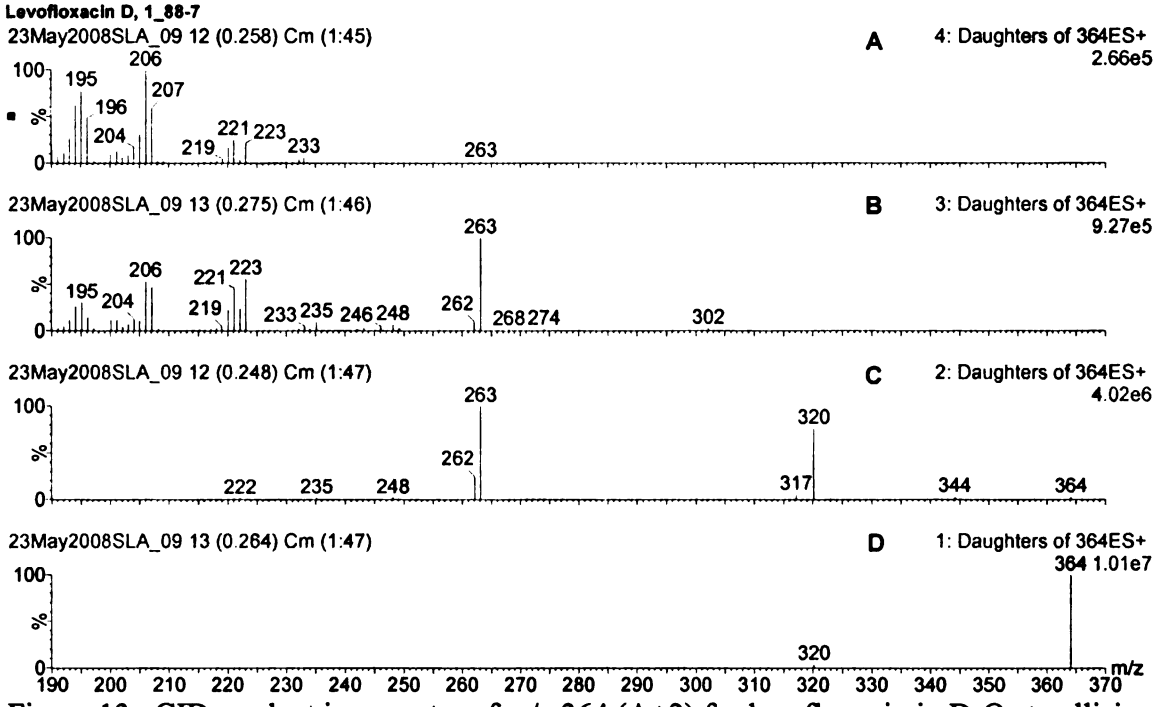

Figure 13. CID product ion spectra of m/z 364 (A+2) for levofloxacin in D_2O at collision cell potentials of (A) 55 V, (B) 40 V, (C) 25 V, and (D) 10 V

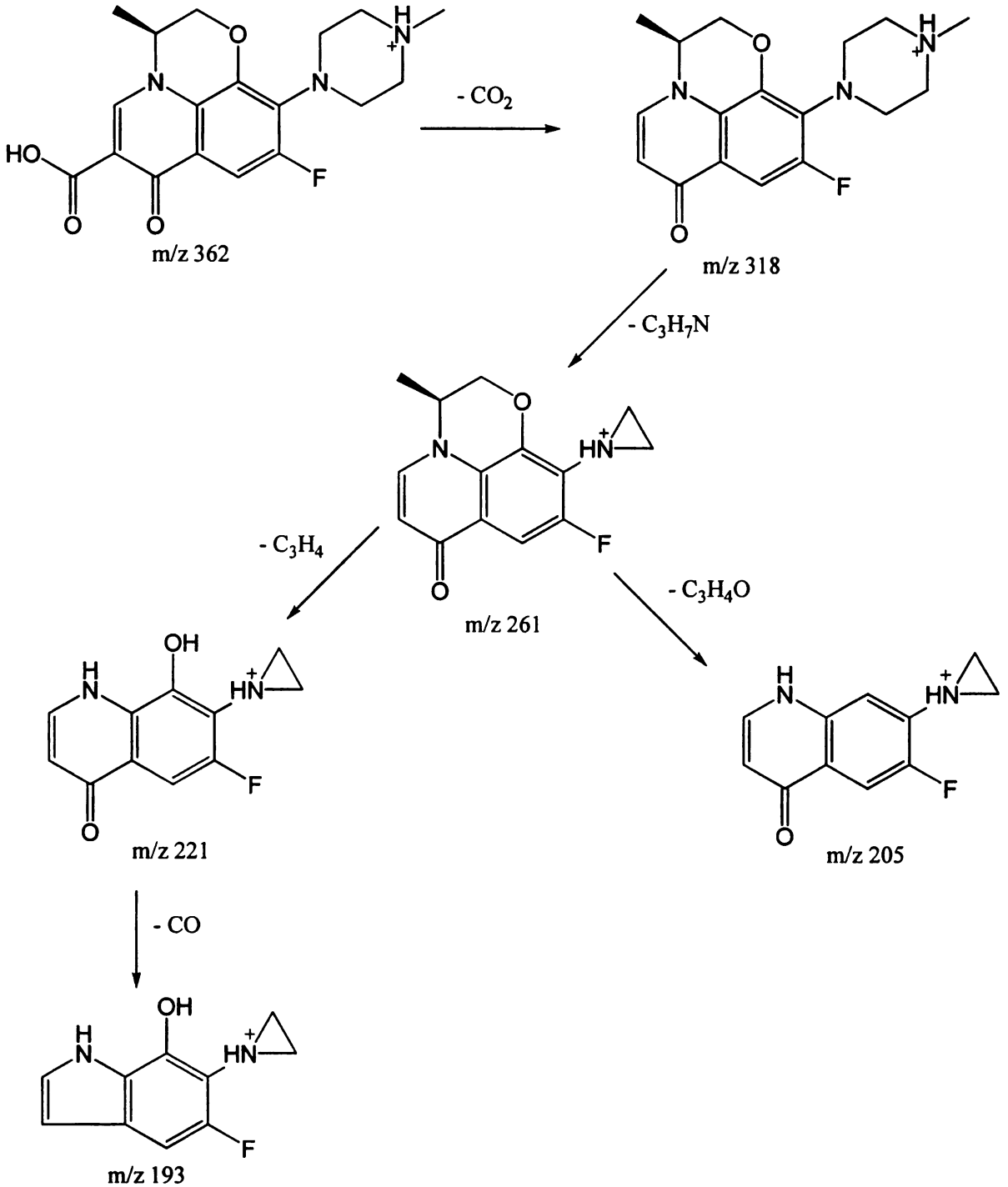

Figure 14. Proposed fragmentation pathway for protonated levofloxacin

CID of protonated levofloxacin (m/z 362) yields loss of water (18 units (u)) from the carboxyl group to give m/z 344 (not shown) or loss of CO_2 (44 u) to give m/z 318.

This loss of CO_2 occurs with simultaneous migration of the hydrogen from the carboxyl group to the fluoroquinolone backbone. CID of deuterated levofloxacin (m/z 364, $[M+D]^+$ for levofloxacin-d_1) also exhibits a loss of 44 u, demonstrating that the deuterium migrates from the carboxyl group to the quinolone backbone, as levofloxacin's only exchangeable hydrogen is located on the hydroxyl group. The fragment at m/z 261 can be explained by loss of C_3H_7N (57 u) from m/z 318. Pseudo-MS^3 experiments generated product ion spectra for m/z 318 (Appendix I, Figure 43), which showed a loss of 57 u from m/z 318. Loss of 57 u, which is attributed to loss of C_3H_7N, is presumed to occur by fragmentation of the piperazine ring, as this is the region of the molecule most likely to contain such hydrogen-rich functionality. CID of deuterated levofloxacin also exhibits a loss of 57 u, suggesting fragmentation of the piperazine ring as no exchangeable hydrogen atoms were involved in this fragmentation (no exchangeable hydrogens are present on the lost portion of the piperazine ring suggesting that an exchangeable hydrogen migrates to remain on the aziridine ring).

The levofloxacin fragment ion at m/z 261 undergoes further fragmentation to give m/z 205 or m/z 221 in pseudo-MS^3 experiments (Appendix I, Figure 44). The latter is a loss of 40 u, attributed to C_3H_4, which would require hydrogen migration from the morpholine ring to the quinolone backbone. The former is the result of a loss of 56 u, attributed to loss of C_3H_4O, which would require migration of two hydrogen atoms from the morpholine ring to the rest of the molecule. The aliphatic portion of the morpholine ring contains six hydrogen atoms. A fragment ion at m/z 205 was also obtained for ciprofloxacin, which will be discussed later in this chapter (Figure 17). D'Agostino et al. [38] observed a similar phenomenon in their CID experiments with levofloxacin

(referred to as ofloxacin) and ciprofloxacin, as well norfloxacin and enoxacin. They observed that various fluoroquinolones studied exhibited similar fragmentation behavior to one another during ESI-MS analysis, including neutral losses of water, CO_2, the cyclic substituent from the pyridine ring, and fragmentation of the piperazine ring. All fluoroquinolones analyzed fragment to yield m/z 205 (or m/z 206 in the case of enoxacin, which contains a nitrogen atom in the fluoroquinolone backbone), the structure of which is shown in Figure 14. This demonstrates that these fluoroquinolones fragment to yield a common structure.

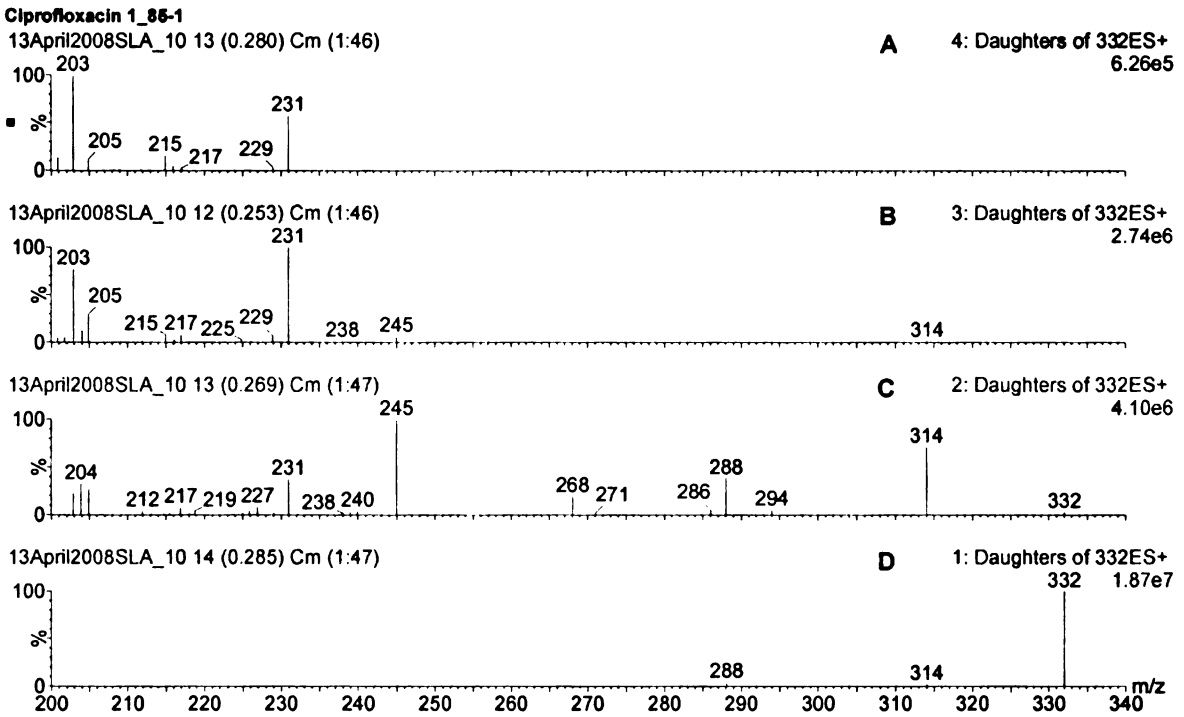

Figure 15. CID product ion spectra for protonated ciprofloxacin (m/z 332) at collision cell potentials of (A) 55 V, (B) 40 V, (C) 25 V, and (D) 10 V

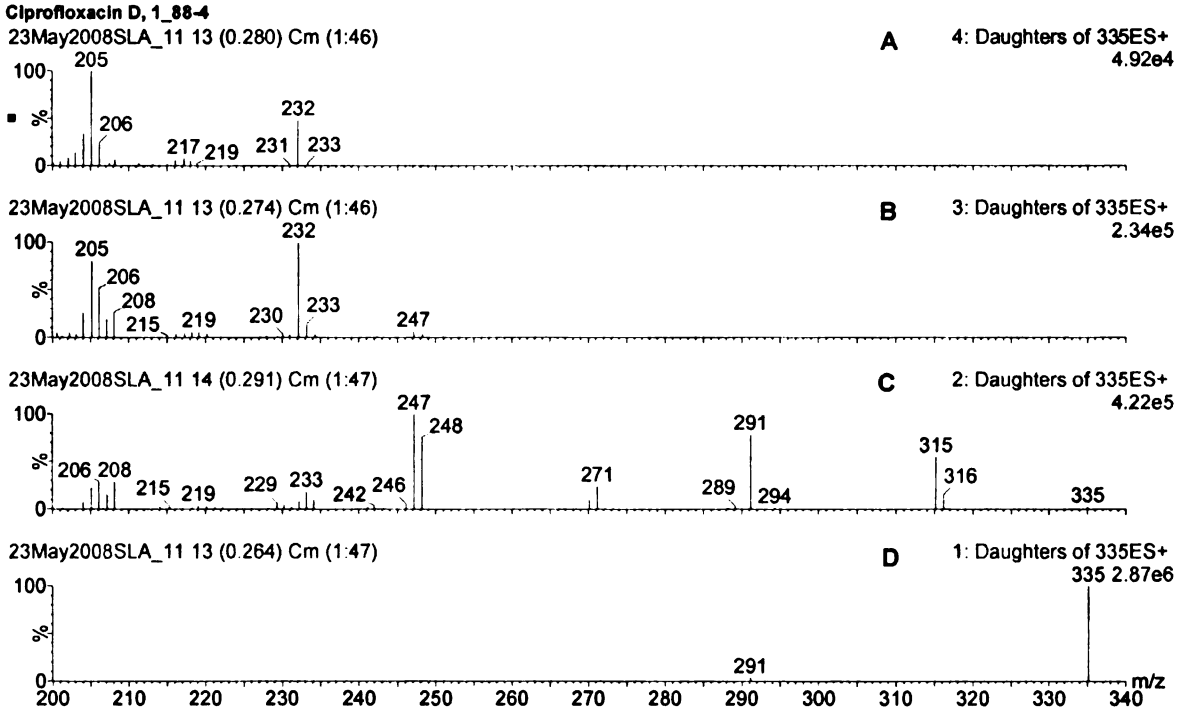

Figure 16. CID product ion spectra of m/z 335 (A+3) in D_2O at collision cell potentials of (A) 55 V, (B) 40 V, (C) 25 V, and (D) 10 V

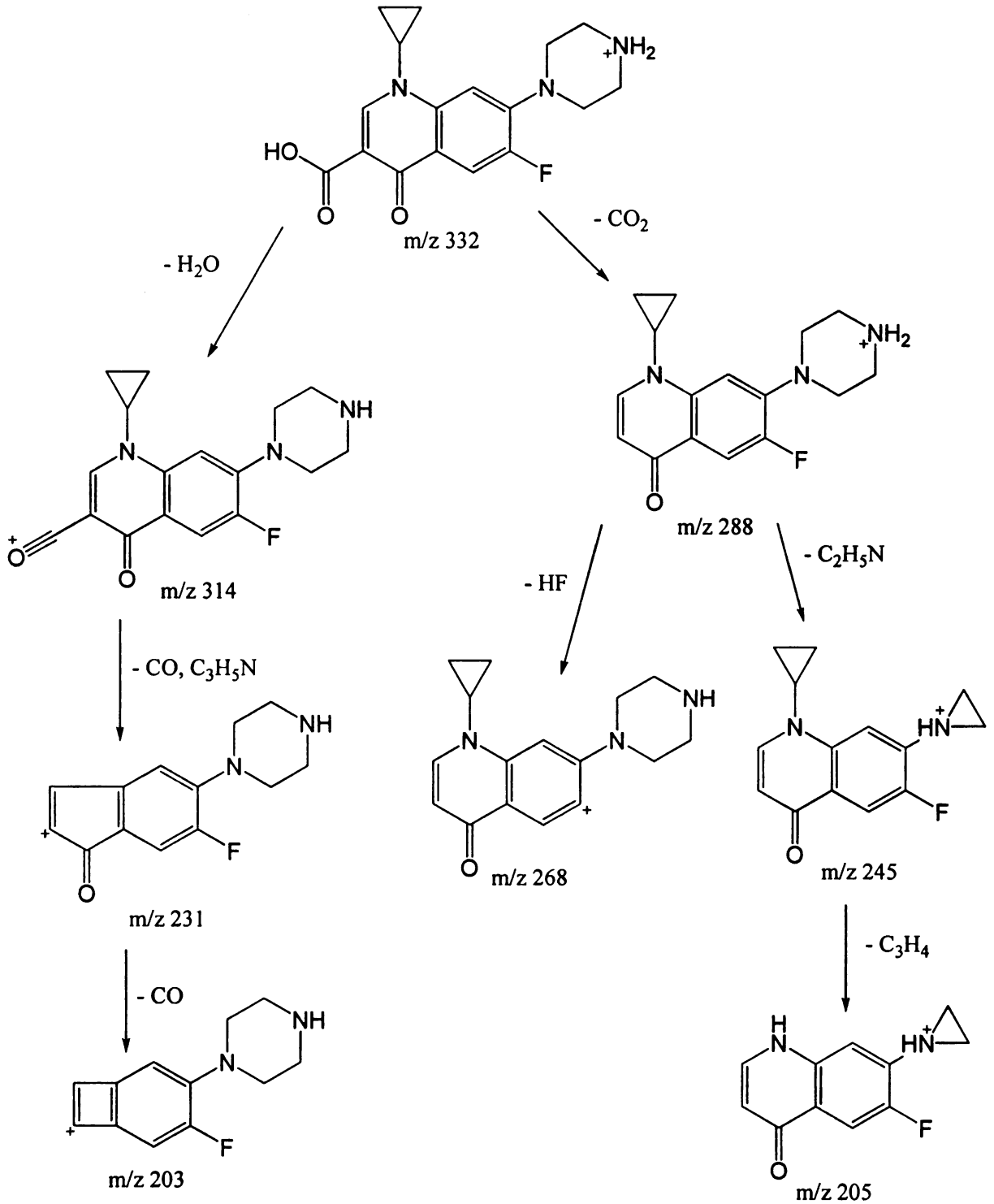

Figure 17. Proposed fragmentation pathways for protonated ciprofloxacin

For CID of protonated ciprofloxacin (m/z 332), loss of either water (18 u) from the carboxyl group to give m/z 314 or loss of CO_2 (44 u) to give m/z 288 are observed. The fragment ion at m/z 314 appears to undergo further fragmentation to give m/z 231, which is attributed to a loss of CO (28 u), followed by a loss of C_3H_5N (55 u), which corresponds to elimination of the cyclopropyl group and attached nitrogen. These losses are also confirmed in pseudo-MS^3 spectra (Appendix I, Figure 45 and Figure 47). As shown in Figure 18, the electrons from the C-C bond between the quinolone backbone and the CO group migrate to the CO group to give an intermediate at m/z 286 (loss of 28 u). This is followed by the migration of electrons from the pyridine ring to the nitrogen, which may insert into the cyclopropane ring to give a neutral fragment of formula C_3H_5N. Since this fragment is neutral, it is not observed in the mass spectra. Further elimination of CO yields a fragment of m/z 203, also shown in Figure 18.

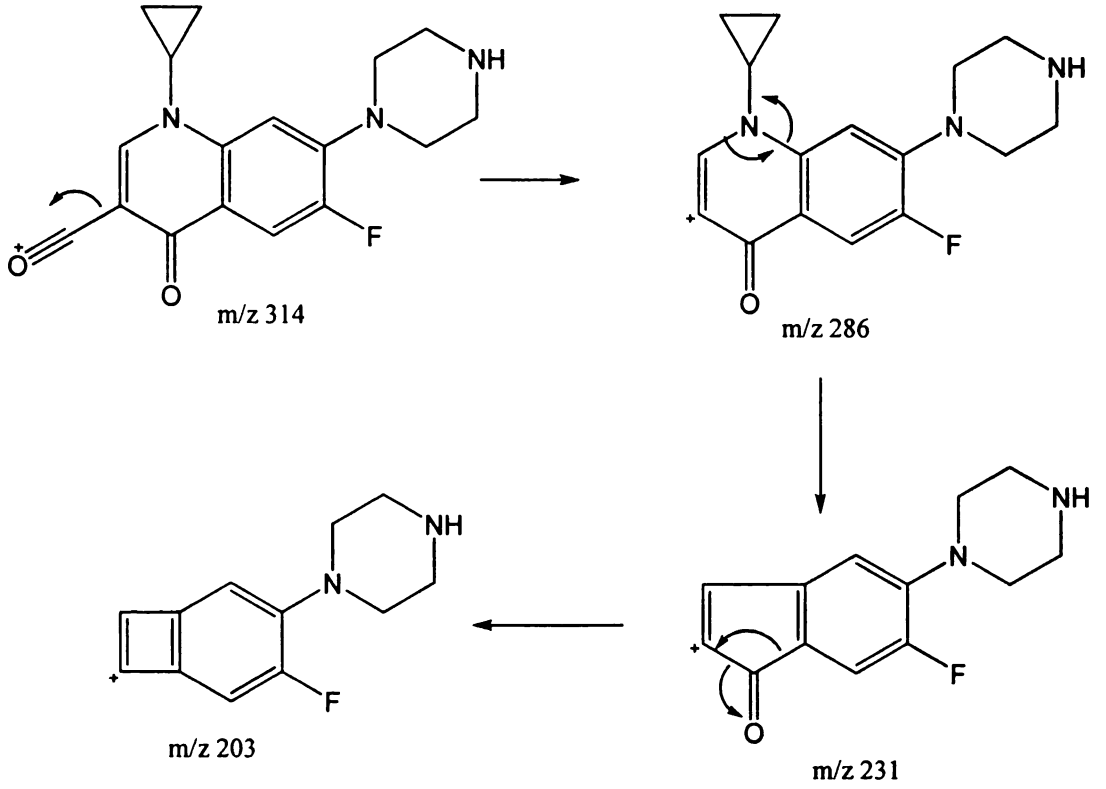

Figure 18. Proposed fragmentation pathway of m/z 314($[M+H-H_2O]^+$ generated by in-source CID of ciprofloxacin ions.

A competing path for fragmentation of protonated ciprofloxacin (m/z 332) results in formation of m/z 288 via the loss of CO_2 (44 u). This must be accompanied by the migration of the hydrogen from the carboxylic acid group to the fluoroquinolone backbone in a manner analogous to levofloxacin. CID of deuterated ciprofloxacin (m/z 335) also exhibits a loss of 44 u, consistent with migration of deuterium from the carboxylic acid group to the fluoroquinolone backbone. Further fragmentation of m/z 288, generated by in-source CID of protonated ciprofloxacin, yields a fragment at m/z 268 corresponding to loss of hydrogen fluoride (20 u) to give m/z 268, or fragmentation of the piperazine ring (43 u) to give m/z 245. In the former case, elimination of HF occurs when a mobile proton combines with the fluorine. This is supported by the loss of

21 u (DF) in deuterated spectra, as opposed to 20 u in protonated spectra, which shows that the deuterium fluoride is lost. This finding suggests that loss of HF in the unlabled ion involves loss of the fluorine plus the proton attached during ionization. For m/z 288, fragmentation of the piperazine ring gives m/z 245 (loss of 43 u). A loss of 44 u (C_2H_4DN) is seen for deuterated spectra (m/z 291 to m/z 247), showing that a deuterium from the piperazine ring leaves as part of C_2H_5N and a deuteron migrates to remain on the aziridine.

For protonated samples of both ciprofloxacin and levofloxacin, fragmentation of the piperazine ring is observed in the forms of m/z 245 for ciprofloxacin and m/z 261 for levofloxacin, shown in Figure 15 and Figure 12 respectively. The losses of water and CO_2 are observed for both protonated molecules as well, and both compounds also lose CO from the pyridinone ring as a loss of 28 u is observed in the protonated spectra of both compounds. Fragmentation of both protonated molecules yields the structure corresponding to m/z 205. The loss of hydrogen fluoride is observed for ciprofloxacin, but not for levofloxacin. This varying fragmentation is a result of one of the structural differences between the two compounds; ciprofloxacin has a cyclopropane substituent on the pyridine ring, whereas levofloxacin has a morpholine ring that cyclizes with the fluoroquinolone backbone. Fewer fragmentation ions are observed for levofloxacin compared to ciprofloxacin, which was also observed by D'Agostino et al. [38], demonstrating that this additional cyclic structure alters the fragmentation of levofloxacin compared to other fluoroquinolones.

Alkali Metal-Cationized Species

The CID mass spectra demonstrate that lithium cationization, compared to protonation, yields different and less diverse fragmentation pathways for both levofloxacin and ciprofloxacin. This is because lithium has a greater mass than a proton, so it migrates across the molecule more slowly than a proton. Many fragmentation pathways with low activation energy involve proton migration. If the migrating proton is the proton attached during ionization, replacing it with a slower-moving lithium ion raises the activation barrier for analogous chemical reactions. The chemical structures shown in this section were drawn to represent the chemical formula of the corresponding m/z values obtained in MS/MS experiments. Since mass spectra do not give unequivocal information about ion structure, details of ion structure should be considered as unproven at present, but the masses suggest elemental compositions of ions.

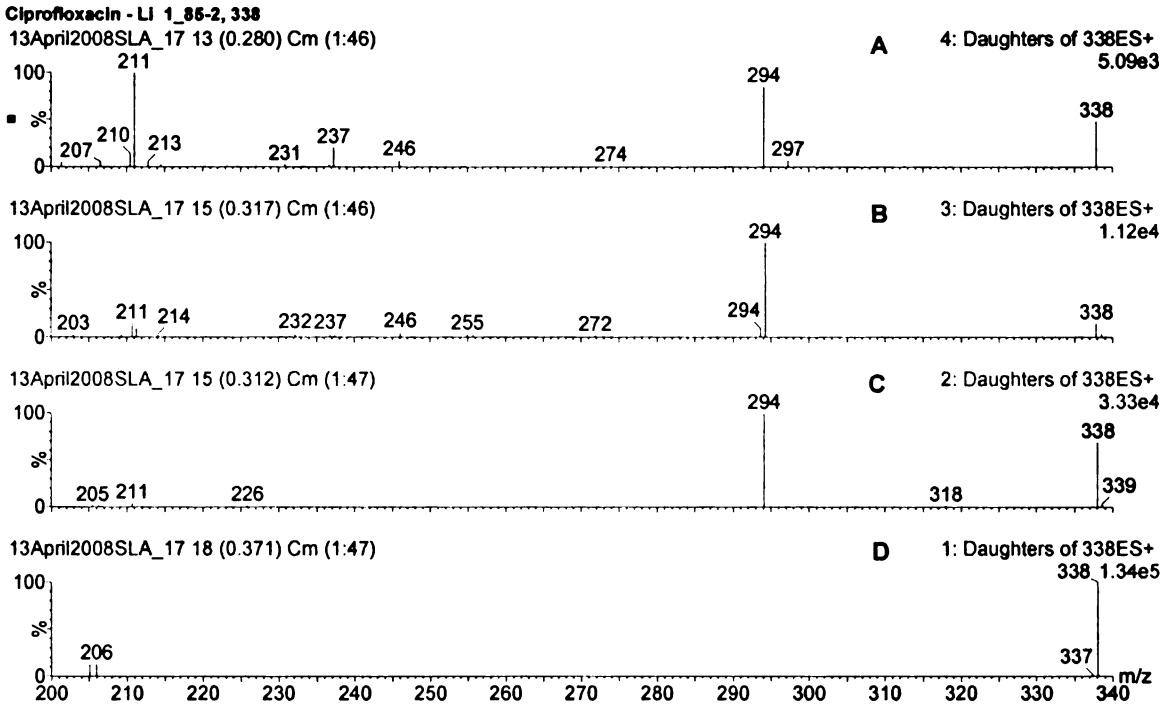

Figure 19. CID product ion spectra of lithium-cationized ciprofloxacin (m/z 338) at collision cell potentials of (A) 35 V, (B) 30 V, (C) 25 V, and (D) 10 V

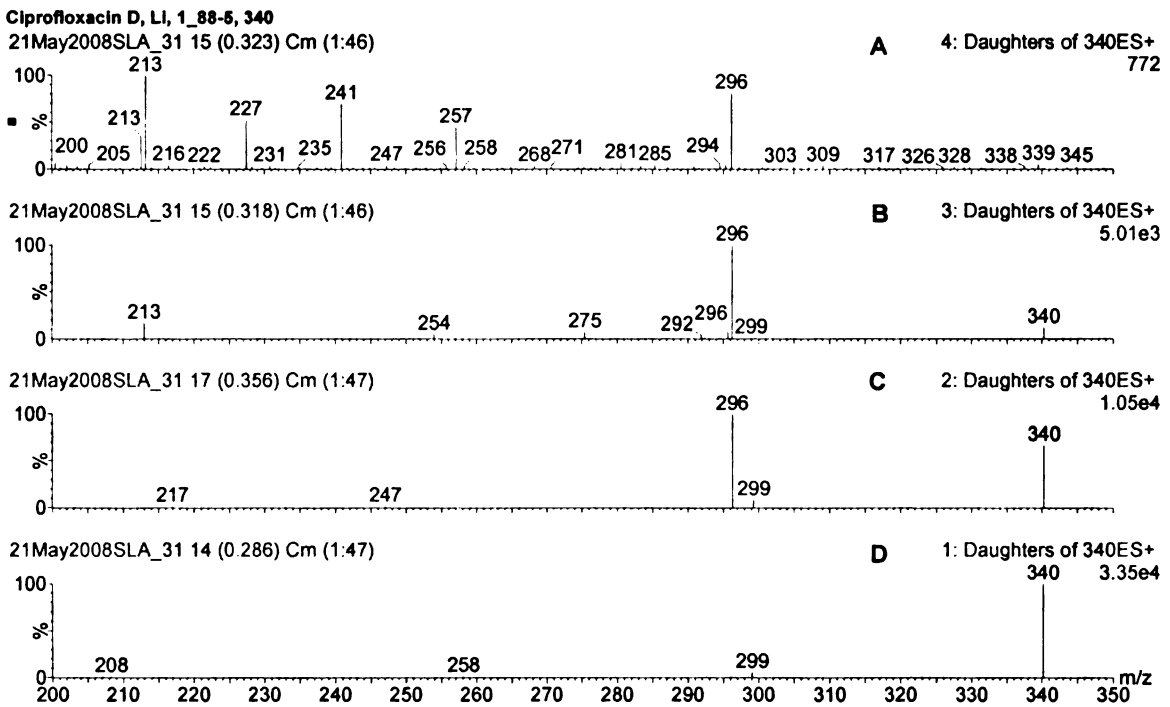

Figure 20. CID product ion spectra of m/z 340 (A+Li+2) in D_2O at collision cell potentials of (A) 35 V, (B) 30 V, (C) 25 V, and (D) 10 V

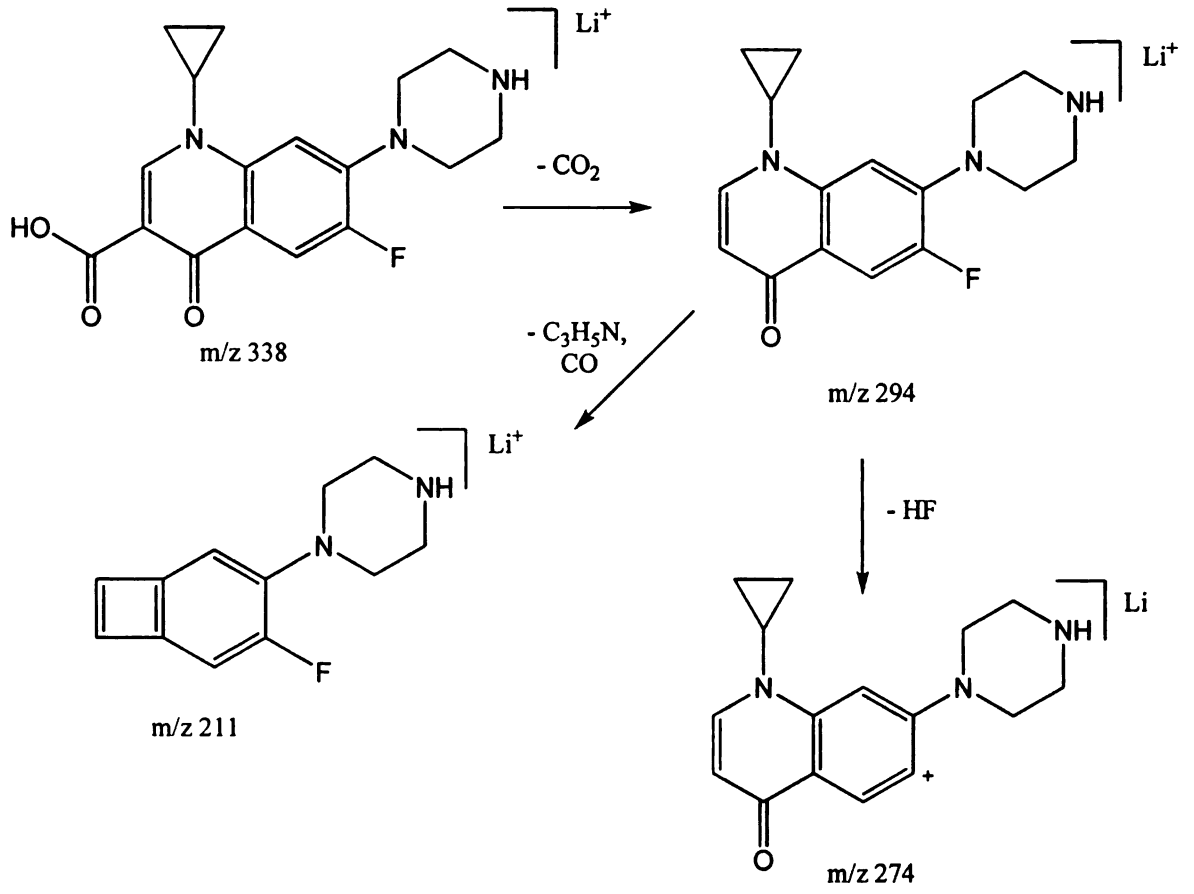

Figure 21. Proposed fragmentation pathways for lithium-cationized ciprofloxacin

For CID of lithium-cationized samples of ciprofloxacin (m/z 338), fragmentation pathways different from those of protonated samples were observed. Unlike protonated samples, no water loss was seen, suggesting that no mobile proton is available to combine with the hydroxyl group, thus inhibiting loss of water. Similar to protonated samples, both C_3H_5N (55 u, from the cyclopropylamine group) and CO (28 u, from the pyridinone) are lost when m/z 294 (the lithiated decarboxylated group) fragments to give m/z 211. CID of deuterated, lithiated ciprofloxacin (m/z 340) exhibits a loss of 83 u (m/z 296 to m/z 213). As loss of 83 u is observed for both deuterated and nondeuterated samples, this suggests that migration of exchangeable hydrogens is not involved in this pathway as the neutral mass loss does not change upon hydrogen-deuterium exchange.

Unlike protonated ciprofloxacin, no fragment ions corresponding to the losses of the neutral species CO and C_3H_5N are observed for lithiated samples. Also, no fragmentation of the piperazine ring was observed (no loss of 43 u), indicating that lithium cationization precludes the hydrogen migration necessary for that fragmentation by interacting with a nitrogen on the piperazine ring. Surprisingly, lithium-cationized ciprofloxacin also loses hydrogen fluoride, which is suggested by H/D exchange experiments. For CID of deuterated, lithiated ciprofloxacin, m/z 296 loses 21 u to give m/z 275, which corresponds to a loss of deuterium fluoride. This behavior might be explained if some of the lithiated molecules consist of a lithium salt of the carboxylate, retaining protonation of the basic piperidine group. The proton attached on the piperidine retains the mobility needed to participate in the elimination of HF. Because lithium has a greater mass than a proton, it migrates more slowly across the analyte molecule, leading to fragmentation pathways that are less diverse then those obtained for protonated samples.

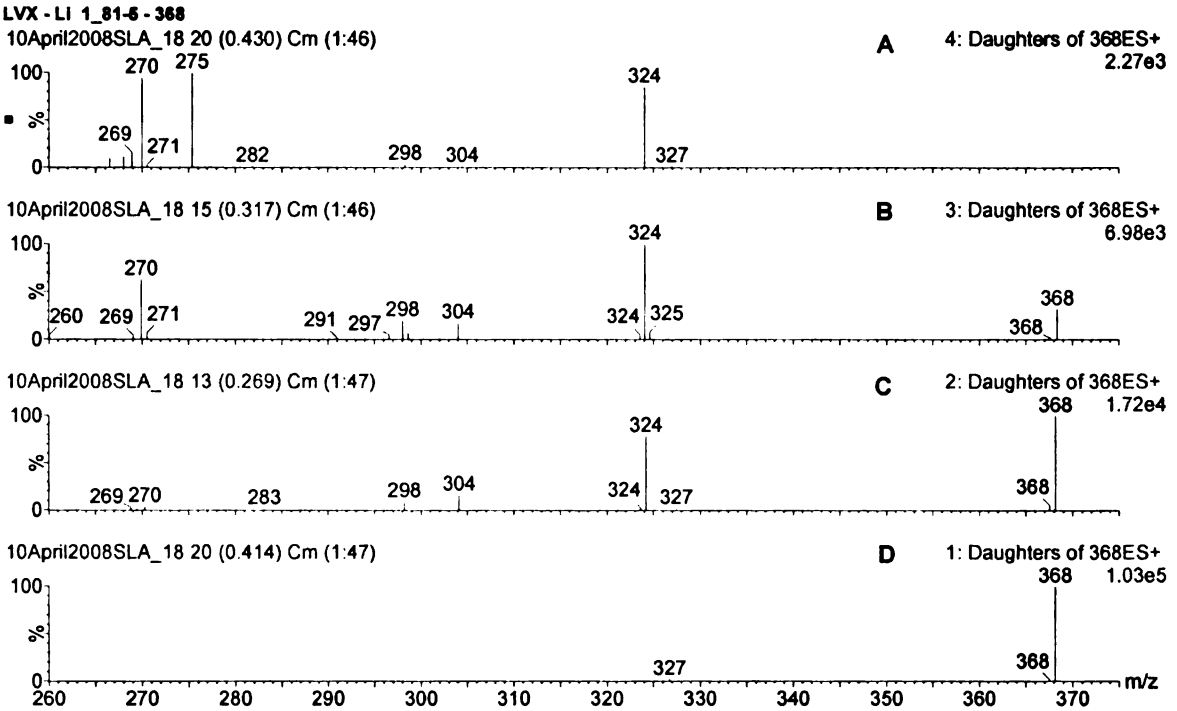

Figure 22. CID product ion spectra of lithium-cationized levofloxacin (m/z 368) at collision cell potentials of (A) 35 V, (B) 30 V, (C) 25 V, and (D) 10 V

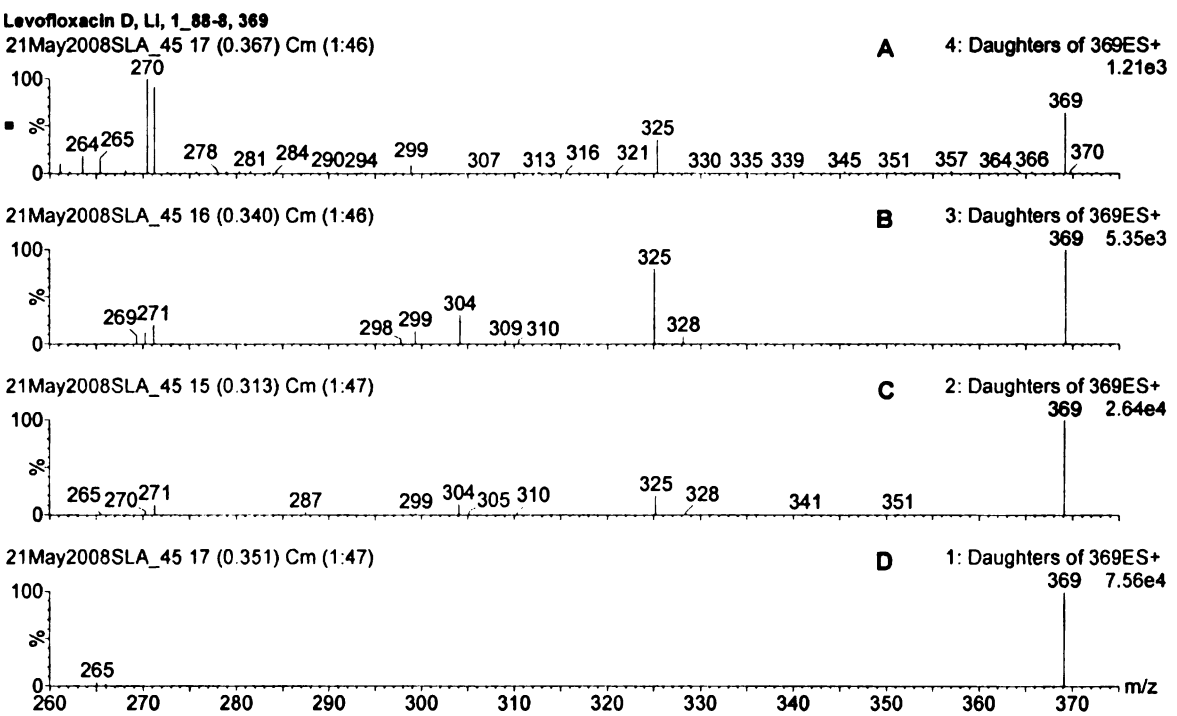

Figure 23. CID product ion spectra for m/z 369 (A+Li+1) for lithium-cationized levofloxacin D_2O at collision cell potentials of (A) 35 V, (B) 30 V, (C) 25 V, and (D) 10 V

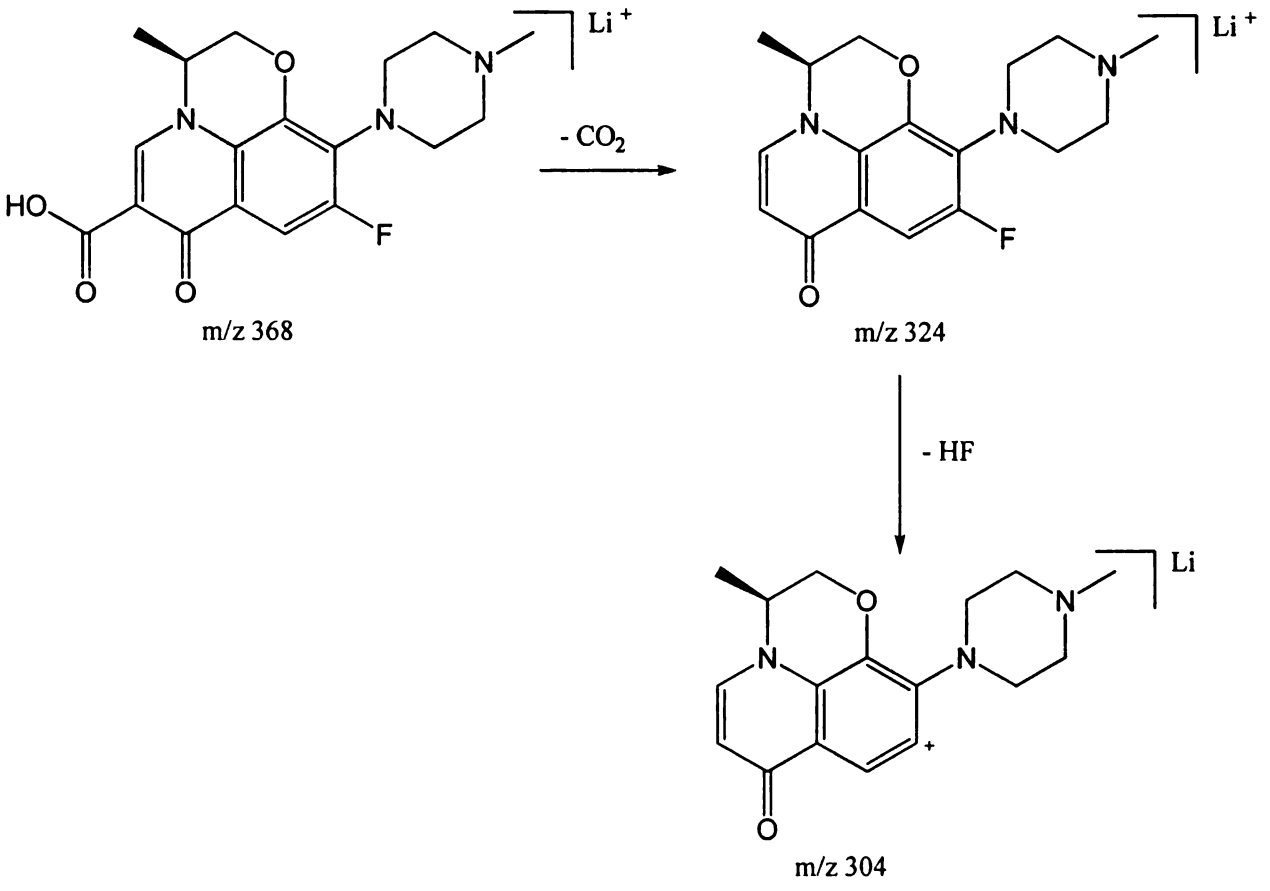

Figure 24. Proposed fragmentation pathways of lithium-cationized levofloxacin

In CID of lithium-cationized levofloxacin (m/z 368), loss of hydrogen fluoride was also observed; this was not observed for protonated samples and provides a fragment unique to lithium cationization. The decarboxylated ion at m/z 324 fragments to give m/z 304, which corresponds to a loss of hydrogen fluoride (20 u). For CID spectra of deuterated, lithiated levofloxacin, a peak at m/z 325 is observed, which loses 21 u to give m/z 304. The loss of 21 u corresponds to a loss of deuterium fluoride. As is the case with both protonated and lithiated ciprofloxacin, the exchangeable hydrogen from the hydroxyl group remains on the quinolone backbone and is lost as hydrogen fluoride for lithiated levofloxacin. Pseudo-MS^3 for which m/z 324 was selected as the parent ion (Appendix I, Figure 49) also suggests that m/z 324 fragments to give m/z 304. Lithium

cationization of levofloxacin is proposed to raise the activation energy needed for competing fragmentation pathways, and allows loss of hydrogen fluoride to become competitive whereas it was not observed for protonated samples. Similar to lithiated ciprofloxacin, no fragmentation of the piperazine ring (no loss of 57 u) was observed, indicating that lithium cationization increases the activation barriers for competing fragmentation reaction, thus allowing the loss of hydrogen fluoride to be detected.

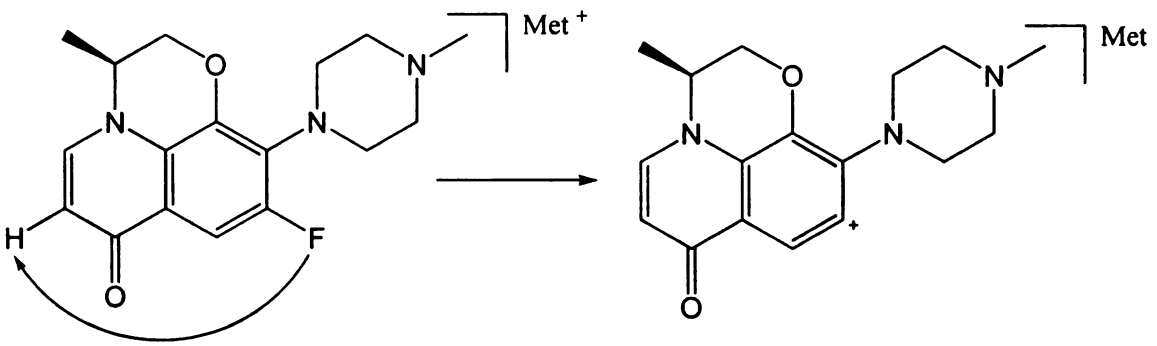

Figure 25. Proposed mechanism for the loss of hydrogen fluoride from levofloxacin, which is not observed for protonated species

Sodium cationization of levofloxacin also results in CID fragmentation different from protonation as it also yields loss of hydrogen fluoride. Since sodium (23 u) has a larger mass than lithium (7 u), it cannot move throughout the molecular surface to the same degree as lithium and therefore pathways that involve either proton or lithium migration will be slower (and less likely to yield observable fragment ions) when these cations are replaced by sodium. Again, loss of HF may involve protonation of the sodium carboxylate salt, retaining a mobile proton needed for HF elimination. Spectra for sodium-cationized fluoroquinolones are shown on the following page.

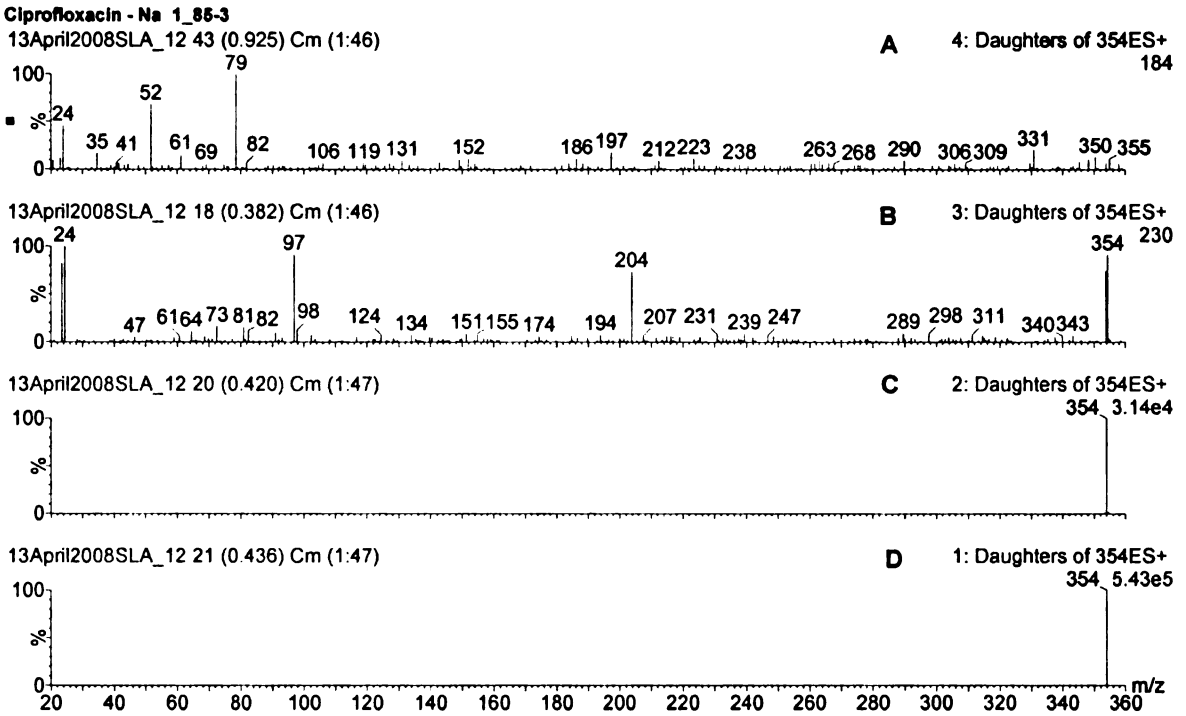

Figure 26. CID product ion spectra of sodium-cationized ciprofloxacin (m/z 354) at collision cell potentials of (A) 35 V, (B) 30 V, (C) 25 V, and (D) 10 V

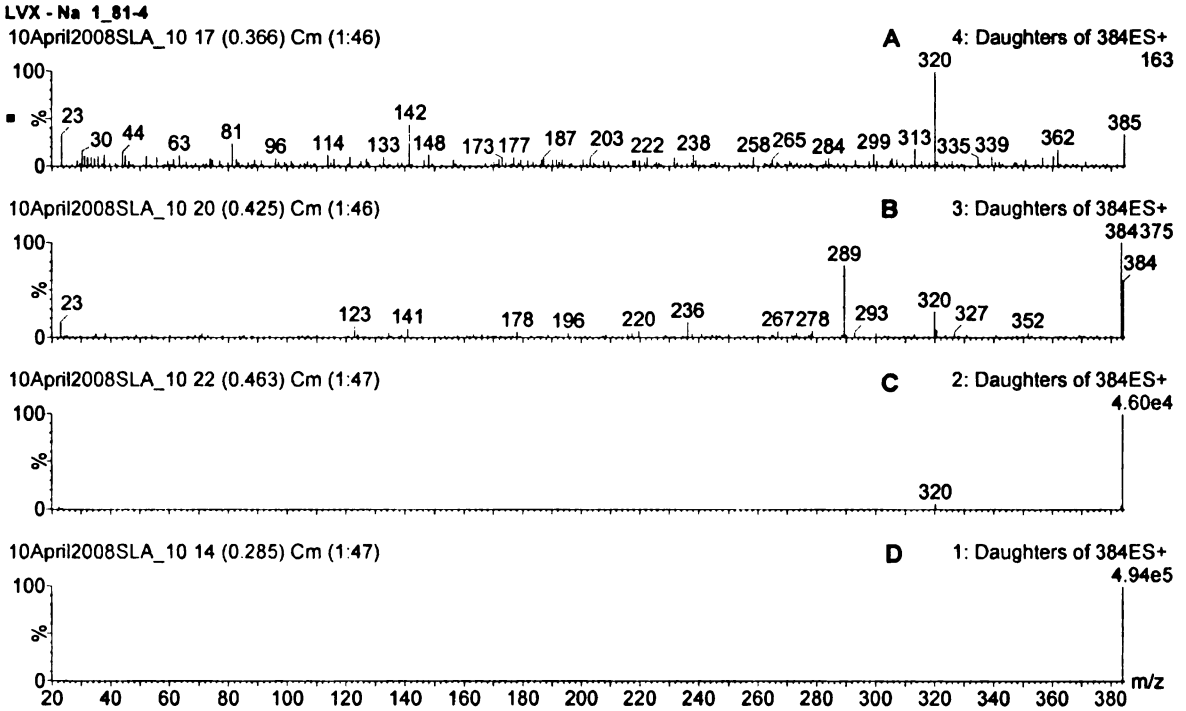

Figure 27. CID product ion spectra of sodium-cationized levofloxacin (m/z 384) at collision cell potentials of (A) 35 V, (B) 30 V, (C) 25 V, and (D) 10 V

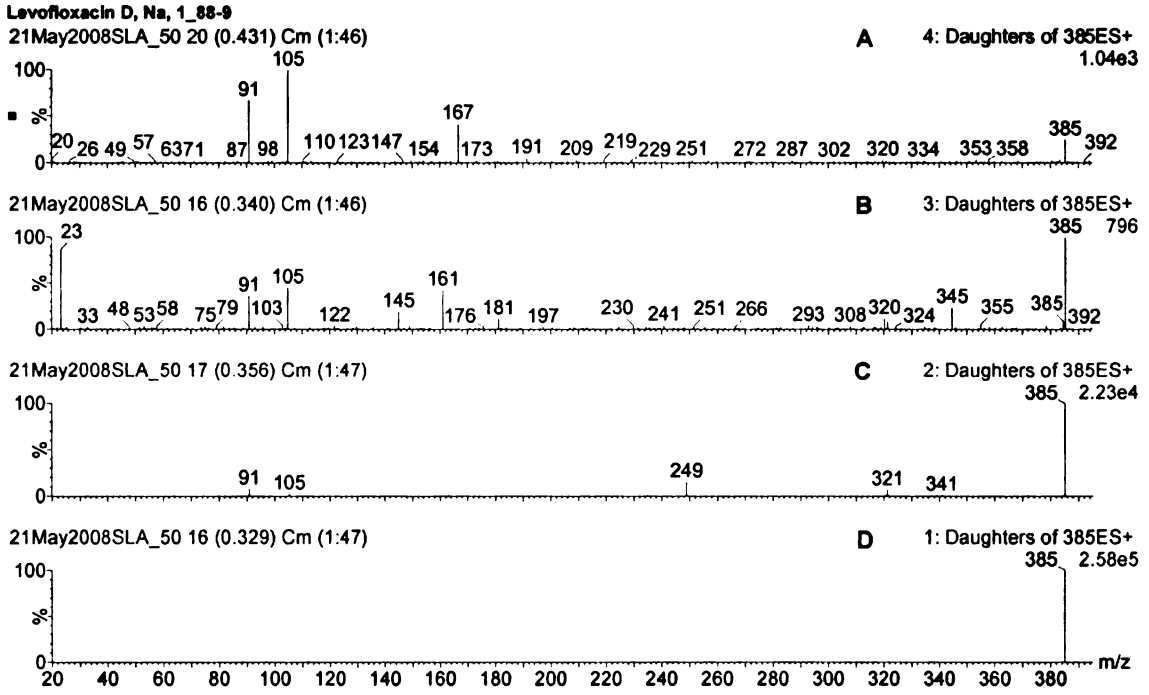

Figure 28. CID product ion spectra of m/z 385 (A+Na+1) for sodium-cationized levofloxacin in D_2O at collision cell potentials of (A) 35 V, (B) 30 V, (C) 25 V, and (D) 10 V

In the case of sodiated ciprofloxacin (m/z 354), the sodium atom (m/z 23) is lost during CID and no fragmentation of the ciprofloxacin molecule itself is observed. Since sodium has a greater ionic radius than lithium, it forms longer bonds with the neutral molecule, therefore its interaction with ciprofloxacin is weaker than that of lithium, causing it to dissociate from ciprofloxacin during CID. In the case of sodiated levofloxacin (m/z 384), loss of 64 u (CO_2 (44 u) and HF (20 u)) yields m/z 320. Analogous to lithiated levofloxacin, the sodium cation may be associated with the carboxylate group, thus precluding the hydrogen migrations necessary to cause a loss of water. A loss 65 u (CO_2 (44 u) and DF (21 u)) to yield m/z 320 is observed for deuterated, sodiated levofloxacin (m/z 385). As with lithiated levofloxacin, sodium cationization of levofloxacin raises the activation energy needed for other competing

fragmentation reactions, allowing loss of hydrogen fluoride to become competive, and gives fragment ions derived from pathways not observed for protonated samples.

For potassium-cationized samples, minimal fragmentation of the compounds is observed. While levofloxacin and ciprofloxacin do form$[M+K]^+$, upon CID of $[M+K]^+$ (m/z 400 and m/z 370 respectively), the $[M+K]^+$ ion is observed at 10 eV, but only K^+ (m/z 39) is observed for the other collision voltages used. This is illustrated in Figure 29. Since potassium has a larger ionic radius than the other cations used, the interaction between it and the two fluoroquinolones is weak, so less energy is needed to cause it to dissociate from the respective compounds.

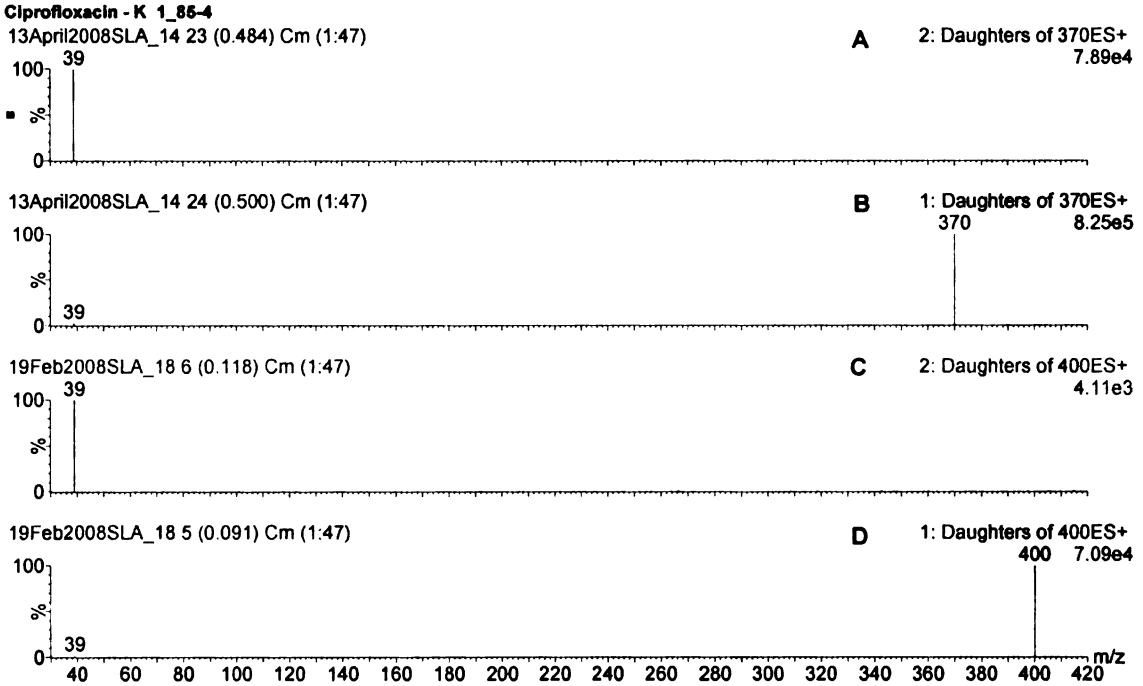

Figure 29. CID product ion spectra of potassium-cationized ciprofloxacin (m/z 370) at collision cell potentials of (A) 25 V and (B) 10 V, and potassium-cationized levofloxacin (m/z 400) at (C) 25 V and (D) 10 V

Discussion

Collision induced dissociation of lithium and sodium ionized species yields the loss of hydrogen fluoride from levofloxacin, a phenomenon that is not observed for protonation, thus providing a method to enhance the fragmentation of levofloxacin. For both ciprofloxacin and levofloxacin, differing fragmentation pathways were achieved using protonation and alkali metal cationization, consistent with a variation in the mobility of the proton, lithium, and sodium. Protonation yielded the most diverse fragmentation because the ionizing proton was able to migrate across the molecule more rapidly than the alkali metal cations. Because lithium and sodium have larger masses than a proton, they cannot migrate across the analyte molecules to the same extent as a proton. As a consequence, some kinds of fragmentation reactions have higher activation barriers and rates of fragmentation too slow to be observed as fragment ions.

Both lithium and sodium cationization yielded loss of hydrogen fluoride, a pathway for levofloxacin not observed with protonation. Lithium and sodium cationization raise the activation energy of competing pathways, allowing loss of HF to become competitive with other fragmentation reactions. For both lithium- and sodium-cationized species, the differing substituents of the fluoroquinolones ciprofloxacin and levofloxacin result in different fragmentation behavior. The additional cyclic component in levofloxacin causes it to yield fewer fragment ions than ciprofloxacin, as was also observed by D'Agnostino et al. [38] .

These experiments demonstrate that lithium and sodium cationization can be used to alter the fragmentation pathways of levofloxacin and ciprofloxacin and reveal the presence of functional groups not evident from the CID of protonated species. While

protonation provides more diverse fragmentation, alkali metal cationization enhances the information in CID spectra of levofloxacin by enabling a loss of hydrogen fluoride. In the case of both analyte molecules, alkali metal cationization increases the activation barrier needed to cause fragmentation of the piperazine ring, thus allowing other fragmentation pathways, such as loss of hydrogen fluoride, to become competitive reaction channels.

While alkali metal cationization of levofloxacin allows observation of the loss of hydrogen fluoride, fragmentation pathways achieved with protonation are more diverse and sometimes more structurally informative. For example, Hemeryck et al. [39] studied the metabolism of levofloxacin in Rhesus monkeys and determined that one of the metabolites produced was desmethyl levofloxacin, a result of the demethylation of the piperazine ring. Analogous to levofloxacin, CID of protonated desmethyl levofloxacin yielded a loss of 44 u (CO_2), which then lost 43 u to give m/z 261. This demonstrates that the methyl group was lost from the piperazine ring rather than the morpholine ring. Since the piperazine ring does not fragment in the case of cationized samples, determining the location of demethylation would be challenging. CID can be applied to the analysis of protonated levofloxacin and ciprofloxacin metabolites to help determine where any structural modifications have occurred during metabolism, thus allowing for the possible determination of the pathways involved in the metabolism of these compounds.

Erythromycin

Protonated Species

Figure 30 and Figure 31 show CID spectra of protonated and deuterated erythromycin, respectively. Figure 32 illustrates the proposed fragmentation pathway for protonated samples of erythromycin. CID of the parent ion m/z 734 yields loss of the cladinose sugar (158 u) and three water losses (18 u per loss) from the macrolide ring (which appear in the spectra at m/z 558, 540, and 522). Loss and subsequent fragmentation of desosamine is observed, with desosamine (m/z 158) undergoing further fragmentation at collision voltages of 40 and 55 eV to give m/z 116 through the loss of 42 u. Protonated desosamine (m/z 158) appears as the dominant fragment owing to its greater basicity than the macrolide ring, which was not observed as a fragment ion. The CID spectra for protonated erythromycin therefore conveys virtually no information about the structure of the macrolide ring, thus limiting the prospects for using CID of protonated species to distinguish positions of any metabolic alterations in erythromycin metabolites or analogs.

Product ion spectra of deuterated erythromycin with five deuterons (m/z 739) exhibits a loss of 159 u (m/z 580), which is attributed to the cladinose sugar as it has one exchangeable hydrogen. The loss of $^{2}H_{1}$-desosamine (m/z 159) and three deuterated water (HDO) losses (19 u per loss) are also confirmed for deuterated, protonated erythromycin samples to give ions at m/z values of 561, 542, and 523.

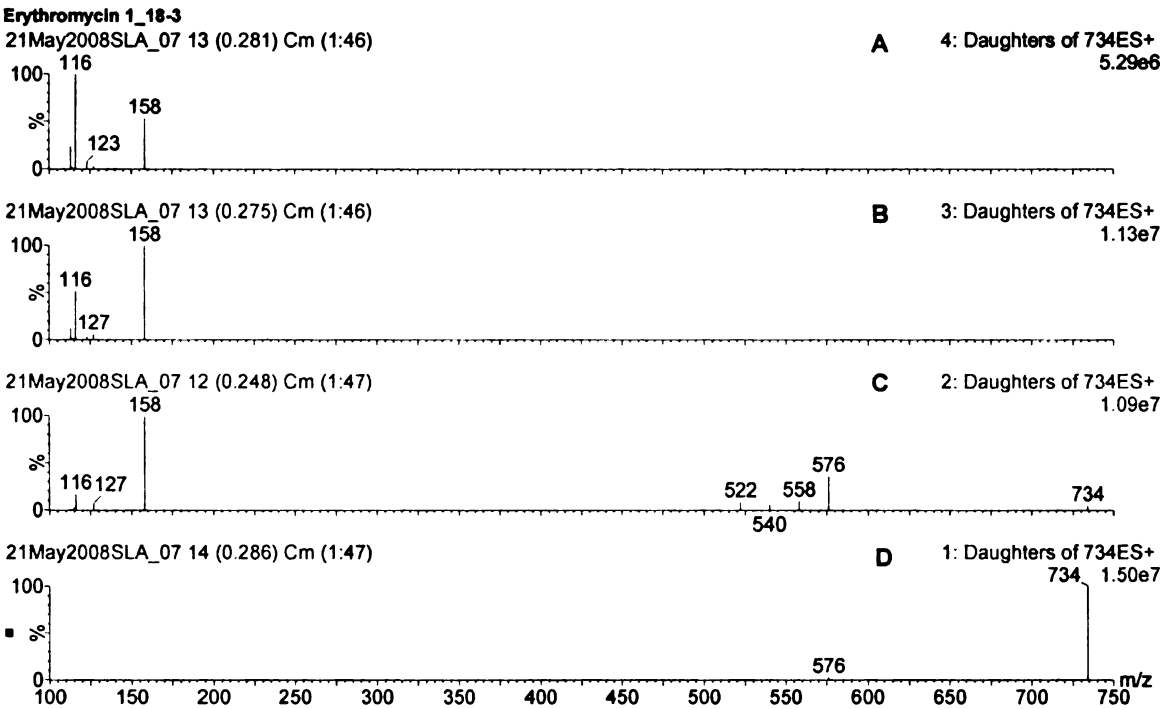

Figure 30. CID product ion spectra of erythromycin (m/z 734) at collision cell potentials of (A) 55 V, (B) 40 V, (C) 25 V, and (D) 10 V

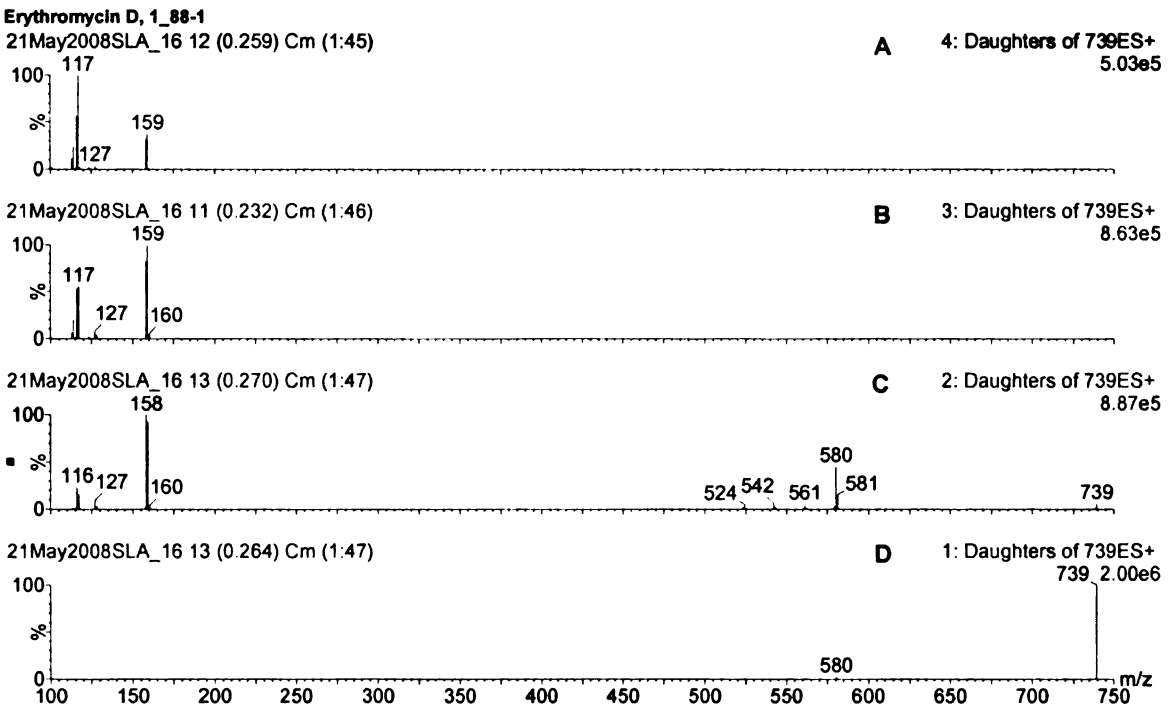

Figure 31. CID product ion spectra of m/z 739 (A+5) of erythromycin in D_2O at collision cell potentials of (A) 55 V, (B) 40 V, (C) 25 V, and (D) 10 V

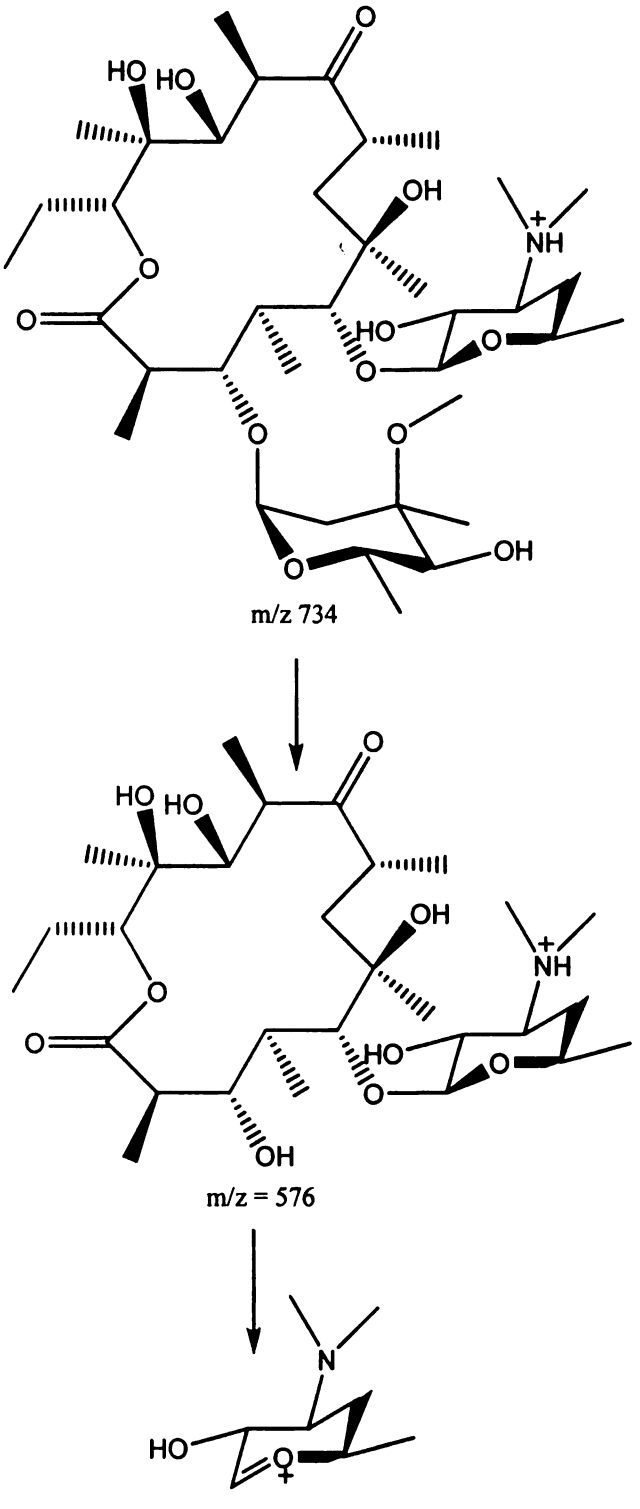

Figure 32. Proposed fragmentation pathway for protonated erythromycin

Alkali Metal-Cationized Species

While CID of protonated erythromycin does not yield ions derived from fragmentation of the macrolide ring, CID of sodium-cationized erythromycin (Figure 33 and Figure 34) causes fragmentation of the macrolide ring (m/z values 423 and 309), thus allowing for the examination any structural alterations that have taken place on the macrolide ring. Fragmentation of the macrolide ring is observed at a collision voltage of 55 eV as seen in Figure 33 on the following page. The chemical structures shown in this section were drawn to represent the chemical formula of the corresponding m/z values obtained in MS/MS experiments.

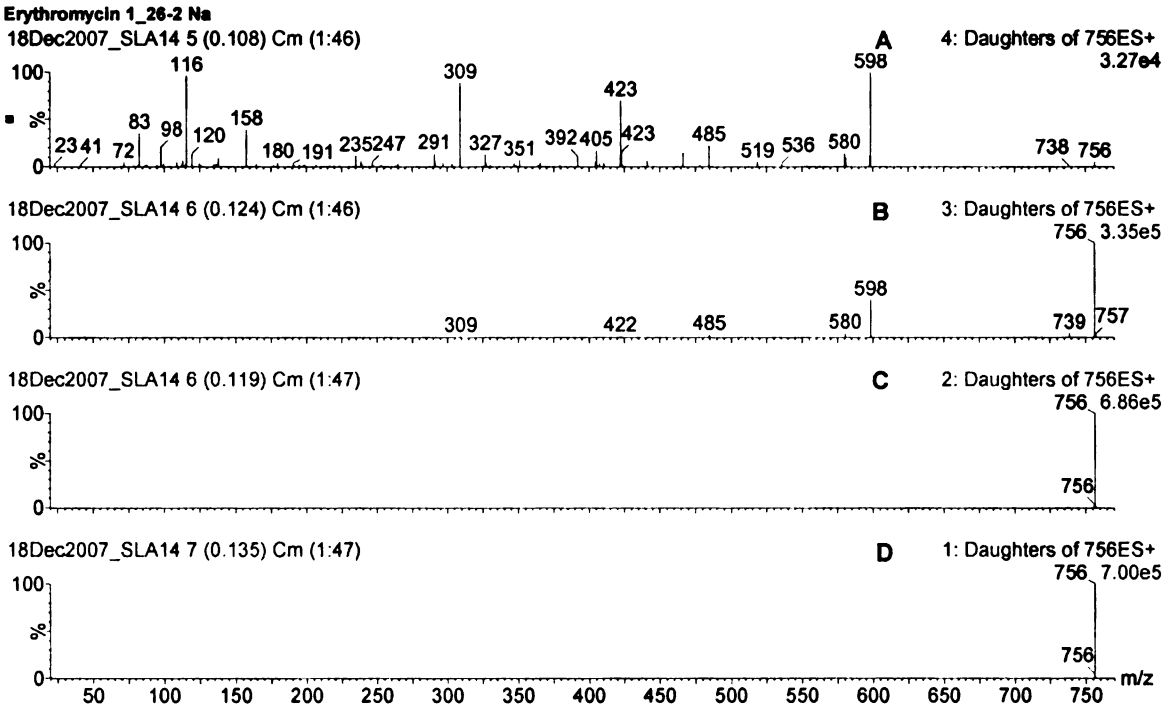

Figure 33. CID product ion spectra of sodium-cationized erythromycin (m/z 756) at collision cell potentials of (A) 55 V, (B) 40 V, (C) 25 V, and (D) 10 V

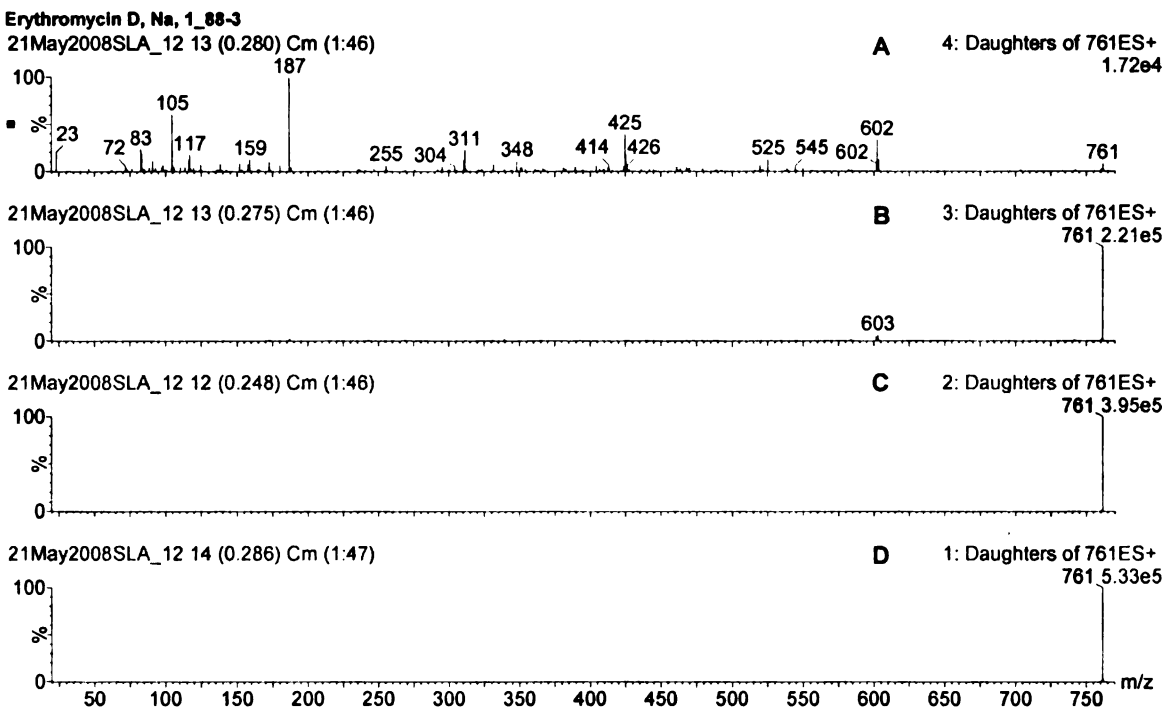

Figure 34. CID product ion spectra of m/z 761 (A+Na+5) for sodium-cationized erythromycin in D_2O at collision cell potentials of (A) 55 V, (B) 40 V, (C) 20 V, and (D) 10 V

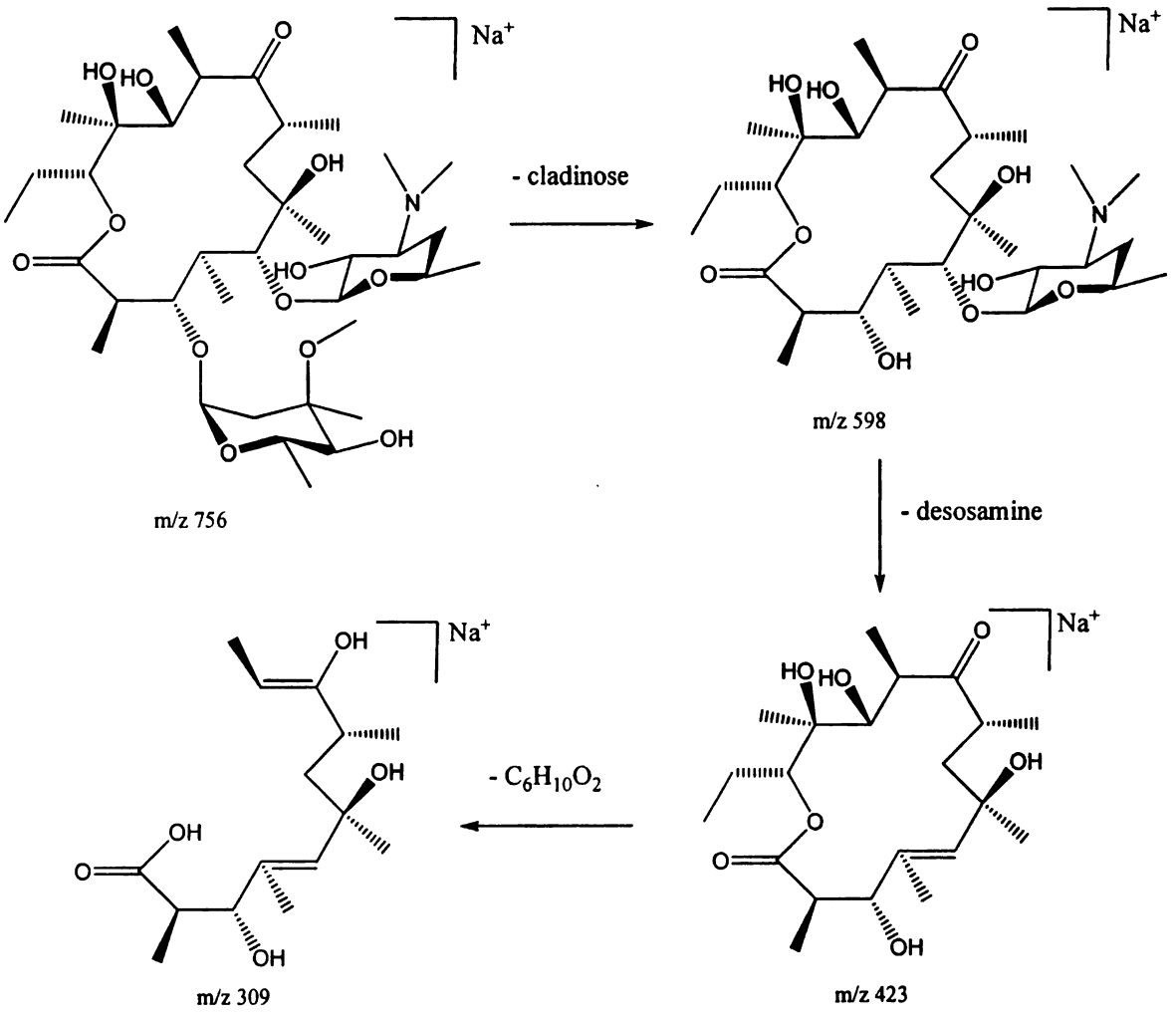

Figure 35. Proposed fragmentation pathway for sodium-cationized erythromycin

CID of sodiated erythromycin (m/z 756) exhibits a loss of 158 u to give m/z 598, which corresponds to loss of cladinose. A subsequent loss of neutral desosamine (175 u) is observed similar to protonated samples. The difference between CID behavior of protonated and sodiated species may be explained by different sites of ionization. In contrast to proton attachment at nitrogen on the desosamine, the sodium cation is expected to form complexes with oxygen substituents on the macrolide ring, giving m/z 423 as a fragmentation product. The macrolide ring can undergo further fragmentation to give m/z 309, attributed to loss of neutral $C_6H_{10}O_2$ (114 u). For CID of deuterated,

sodiated erythromycin, a loss of 115 u is observed, giving m/z 311. This demonstrates that one exchangeable hydrogen is lost, while another migrates and remains with the macrolide ring as there is a mass shift of one for the neutral loss (114 and 115 u) and a mass shift of two for the remaining fragment (m/z 309 and 311), which only has one exchangeable hydrogen. A proposed mechanism for this phenomenon is shown in Figure 36. CID of sodium-cationized samples of erythromycin yields fragmentation of the macrolide ring, which is not observed for CID of protonated erythromycin samples.

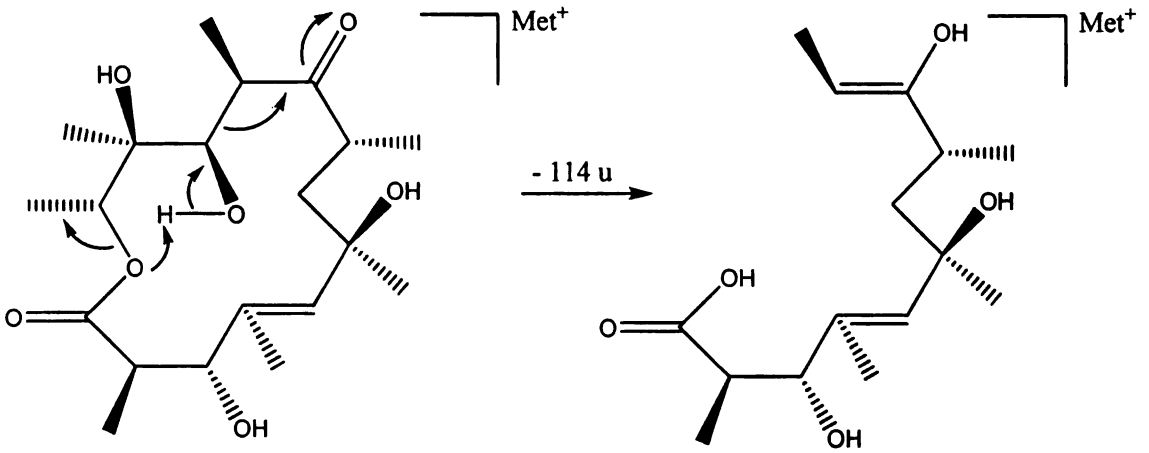

Figure 36. Mechanism for the loss of 114 u from the macrolide ring of erythromycin

Proposed structures for sodium-cationized erythromycin were confirmed by pseudo-MS^3 analysis. For these experiments, m/z 309 was selected as the parent ion for CID (Appendix I, Figure 50). The proposed fragmentation pathway for m/z 309 is illustrated in Figure 37 on the following page.

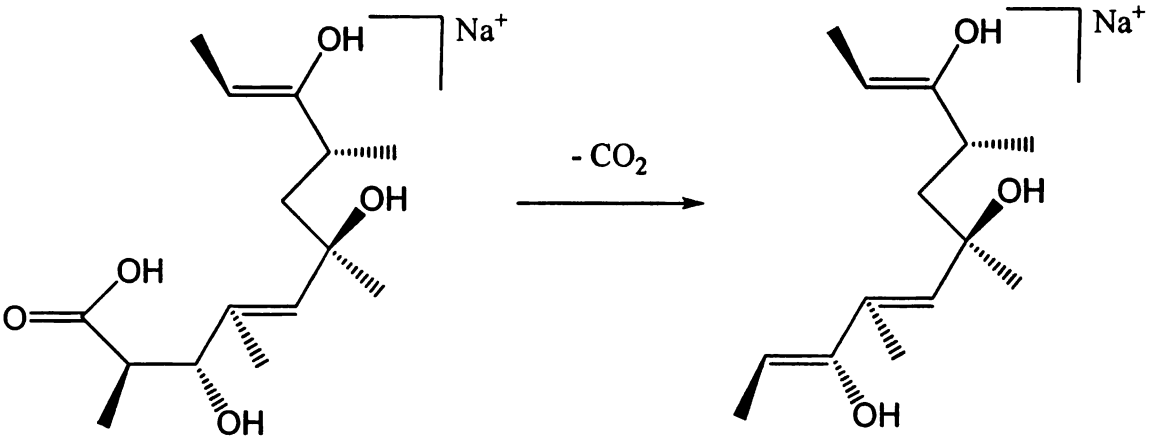

m/z 309 m/z 265

Figure 37. Proposed fragmentation pathway of m/z 309

Lithium-cationization yields different fragmentation pathways and further fragmentation of the macrolide ring compared to protonated and sodium-cationized samples of erythromycin (Figure 38 and Figure 39. Unlike sodium-cationized samples, desosamine is not lost as a neutral sugar in the case of m/z 520 and m/z 468. This behavior is interpreted as being similar to the phenomenon seen in protonated spectra, with the lithium cation attached at the nitrogen on the desosamine in these cases, as desosamine is not lost (as a neutral of 175 u from the lithiated species). Since lithium has a lesser mass than sodium, it is more mobile, allowing it to interact with either the nitrogen on the desosamine or a carbonyl oxygen on the macrolide ring. The ion resulting from loss of cladinose, m/z 582 can lose either 62 u, attributed to a loss of CO_2 (44 u) and water (18 u), to give m/z 520, or 114 u to give m/z 468 through fragmentation of the macrolide ring, as was discussed in the case of sodium cationization.

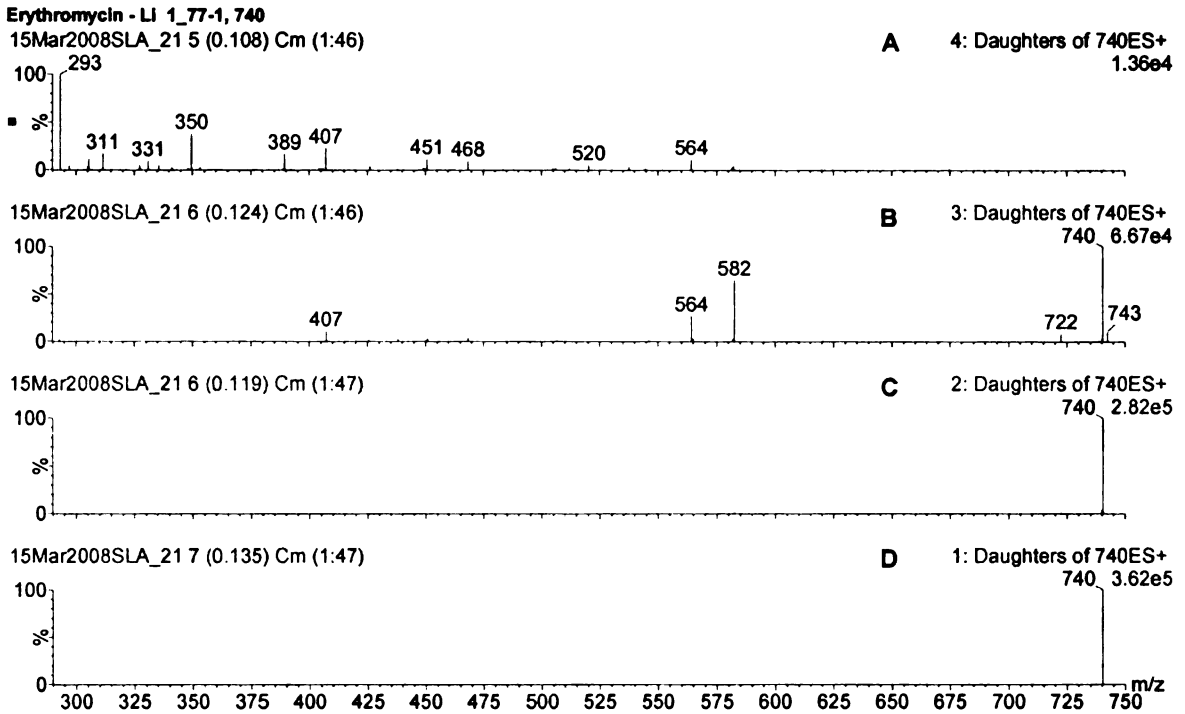

Figure 38. CID product ion spectra of lithium-cationized erythromycin (m/z 740) at collision cell potentials of (A) 55 V, (B) 40 V, (C) 25 V, and (D) 10 V

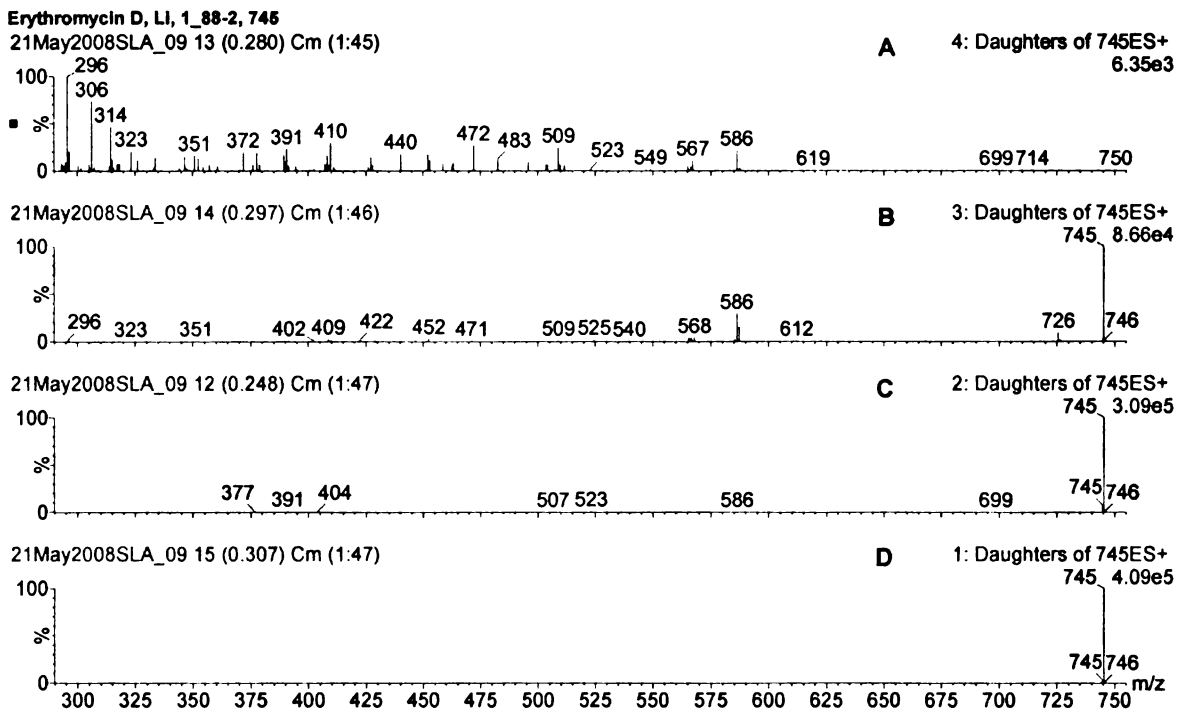

Figure 39. CID product ion spectra of m/z 745 (A+Li+5) for lithium-cationized erythromycin in D_2O at collision cell potentials of (A) 55 V, (B) 40 V, (C) 25 V, and (D) 10 V

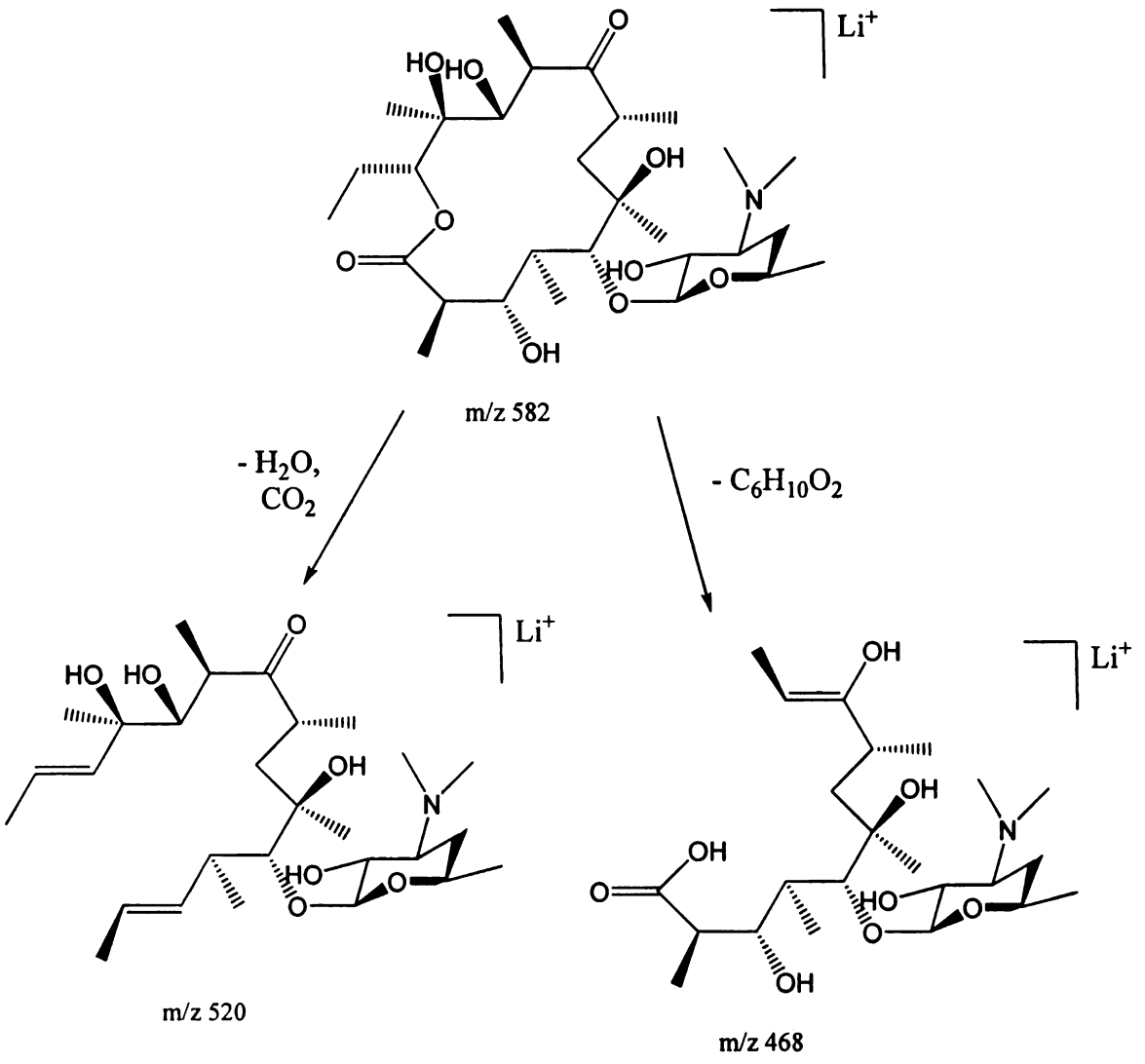

Figure 40. Proposed fragmentation pathways of m/z 582

While a loss of 114 u ($C_6H_{10}O_2$) from the macrolide ring was also observed for sodium-cationized erythromycin, a loss of 62 u is unique to lithium-cationized species. This loss of 62 u is attributed to a loss of water (18 u) from the macrolide ring to give m/z 564 (structure not shown), followed by a loss of CO_2 (44 u) from the macrolide ring to give m/z 520 (Figure 40). For CID of deuterated, lithiated erythromycin (m/z 745), a loss of deuterated water (19 u, HDO) from m/z 586 to give m/z 567 is observed followed by a loss of 44 u to give m/z 523. Because a loss of 44 u is also observed for lithiated

erythromycin, this demonstrated that no exchangeable hydrogens are involved in the loss of 44 u. In pseudo-MS^3 spectra for which m/z 582 was selected as the parent ion (Figure 51), peaks at m/z 293 and m/z 450 (468 – water) were observed, thus demonstrating that these ions result from the fragmentation of m/z 582 and not via some alternative pathway.

For CID of lithiated erythromycin (m/z 740), loss of the cladinose sugar is observed (158 u), similar to both protonated and sodium-cationized samples. A portion of the proposed fragmentation pathway is illustrated in Figure 41. As with sodium-cationized samples, a loss of 114 u, which is attributed to $C_6H_{10}O_2$, from the macrolide ring is observed. From m/z 582 to m/z 468, a loss of 114 u is observed and a loss of 115 u is observed in CID spectra of deuterated, lithiated erythromycin (m/z 745). Similar to sodium-cationized samples, this demonstrates that one exchangeable hydrogen is lost, while another migrates and remains with the macrolide ring, according to the mechanism in Figure 36. The same phenomenon is observed for m/z 407, which loses 114 u to give m/z 293. A loss of 115 u is also observed for deuterated analogs. Like sodium-cationized samples, the lithium is interacting with a carbonyl oxygen on the macrolide ring.

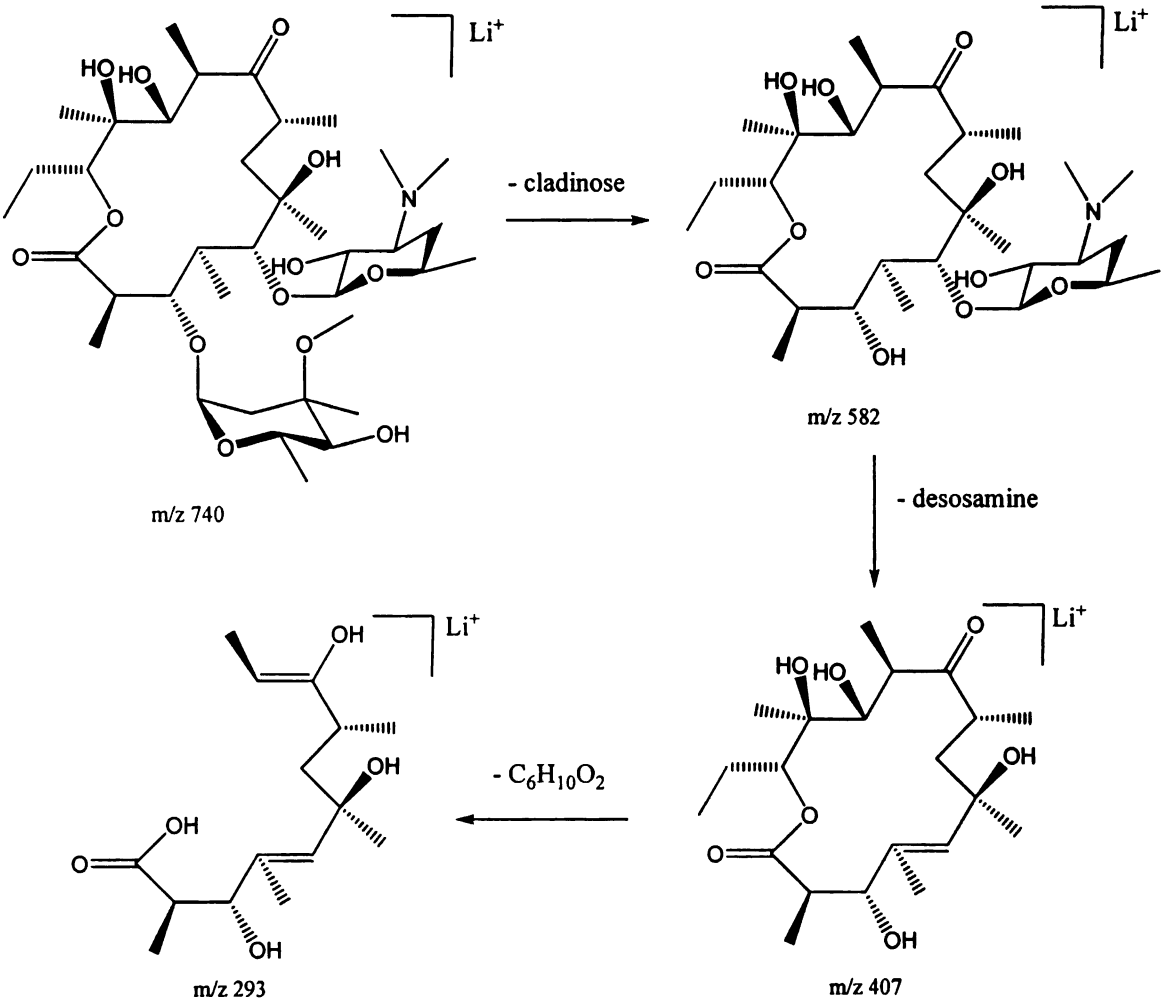

Figure 41. A portion of the proposed fragmentation pathway for lithium-cationized erythromycin

Figure 42 shows the CID spectra for potassium-cationized erythromycin (m/z 772). Only the $M+K^+$ ion (m/z 772), m/z 614 (loss of cladinose, 158 u) and the potassium cation itself (m/z 39) are observed. Because potassium has a greater mass than the other cations used, it cannot migrate across the molecule to the same extent as the other cations. Futhermore, its large ionic radius gives weaker interaction with the erythromycin molecule, thus yielding less fragmentation except for the formation of an abundant potassium cation.

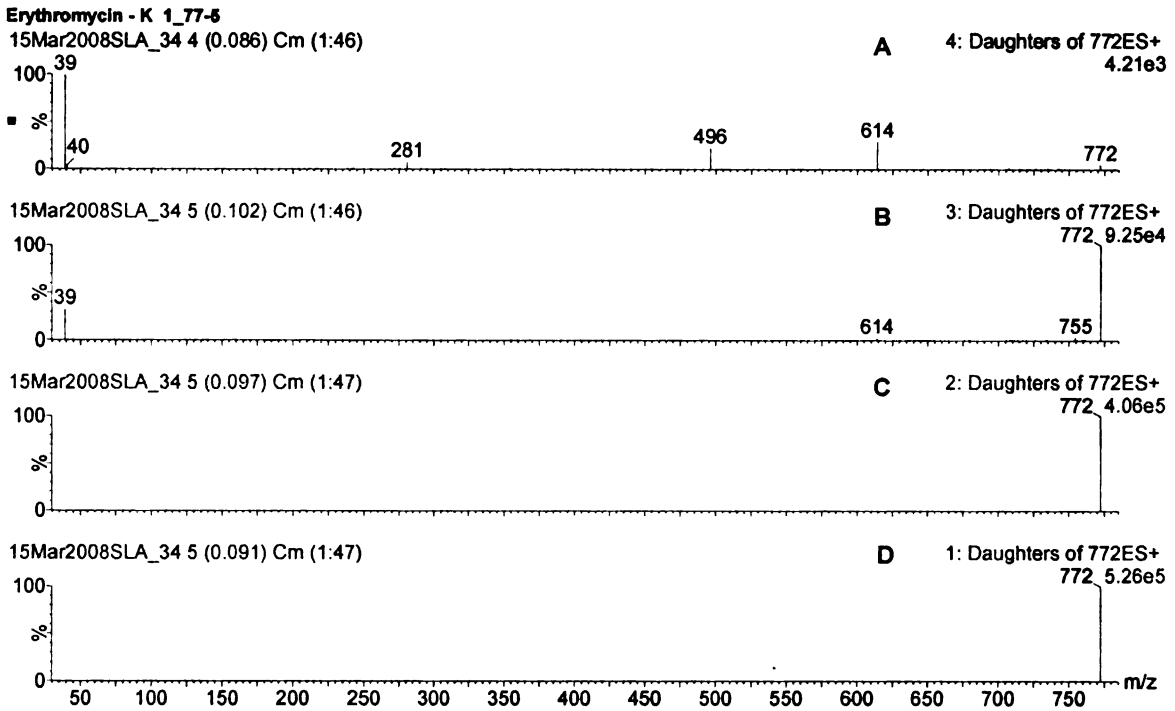

Figure 42. CID of potassium-cationized erythromycin (m/z 772) at collision cell potentials of (A) 55 V, (B) 40 V, (C) 25 V, and (D) 10 V

Discussion

Alkali metal cationization of erythromycin allows cross-ring fragmentation of the macrolide ring that is not obtained from protonated species. This finding suggests that CID of cationized erythromycin can be a useful approach for the structural elucidation of erythromycin metabolites. The varied fragmentation pathways achieved using protonation and alkali metal cationization demonstrate that cationization alters hydrogen migration across the molecule, and alters the fragmentation behavior of the ionized molecule. Both lithium and sodium cationization increase the activation barrier for other fragmentation pathways, allowing for the fragmentation of the macrolide ring to be observed. In the case of potassium cationization, the potassium ion has a greater mass

than other ions, and does not migrate throughout the analyte molecule to the same extent to allow of an array of fragment ions. Also, the size of the potassium ion makes the interactions between it and erythromycin weak compared to the interactions seen with the other cations studied. As a result, when enough energy is applied to potassium-cationized erythromycin, the potassium ion dissociates from the molecule and minimal fragmentation of the analyte molecule is observed. Unlike the fluoroquinolones, fragmentation of the analyte molecule itself is observed in the case of erythromycin (m/z 614 corresponds to $[M+K\text{-cladinose}]^+$).

In the case of protonation, the charge is able to migrate across the erythromycin molecule more than the lithium- and sodium-cationized species because it has a smaller mass than the alkali metal cations and can therefore migrate faster. For the lithium- and sodium-cationized species, the altered charge localization allows for different hydrogen migrations (based upon H/D exchange experiments), and thus different fragmentation pathways. For example, hydrogen migrations for protonated erythromycin caused water losses, while hydrogen migrations for cationized erythromycin caused fragmentation of the macrolide ring. Lithium cationization yields different fragmentation of the macrolide ring compared to sodium cationization because the sodium ion has a larger mass than the lithium ion and therefore the charge cannot migrate as rapidly to participate in transition states to fragmentation.

Also, because the desosamine group is present in some proposed structures for the fragmentation of lithium-cationized species, this suggests that the lithium cation is capable of attachment at with both the nitrogen on the desosamine and the oxygen-containing groups on the macrolide ring. Sodium cationization yields loss of both

cladinose and desosamine, suggesting that the sodium cation is interacting with the carbonyl oxygens on the macrolide ring. Because lithium and sodium have greater masses than a proton, they migrate across the molecule more slowly than a proton, which allows them to be more selective about the sites on the molecule with which they interact.

For erythromycin, lithium and sodium cationization can be used to fragment the macrolide ring and thus help determine the location of any structural modifications that have occurred on that portion of the molecule during the course of metabolism. Sodium and lithium cationization alter the dissociation pathways of erythromycin, thus yielding fragmentation of the macrolide ring, a phenomenon not observed for protonated erythromycin. Because cationization causes fragmentation of the macrolide ring, rather than having it be lost at a neutral in the case of protonation, the macrolide ring can be observed in MS spectra, allowing for the structural elucidation of erythromycin metabolites. As a result, both of these alkali metal cations can be used to enhance the fragmentation of erythromycin and aid in the identification of the position of any structural alterations that have occurred during the metabolism of erythromycin and its analogs.

CHAPTER 3: CONCLUSIONS AND FUTURE WORK

Summary and Conclusions

When used with ESI-MS/MS analysis, alkali metal cationization provides a method to control the fragmentation pathways of pharmaceutical compounds during CID. This concept has been demonstrated in this thesis for the compounds erythromycin and levofloxacin. For both of these compounds, alkali metal cationization yields fragmentation pathways that are not observed for protonated samples. For example, lithium and sodium cationization of levofloxacin allow loss of hydrogen fluoride to be observed, a phenomenon not observed for protonated samples. This allows detection of fluorine substitution to be established. While protonation of erythromycin does not yield fragments indicative of substitution locations on the macrolide ring, both lithium and sodium cationization enable cross-ring fragmentation of the macrolide ring to take place. This has also been observed in previous work investigating the structural elucidation of erythromycin analogs and protecting groups used during their synthesis [40-42]. In the case of erythromycin, the fragmentation obtained using alkali metal cationization provides a means of enhancing fragmentation and determining the location of structural modifications that have been made to the molecule during the course of metabolism.

For erythromycin, levofloxacin, and ciprofloxacin, as the mass of the alkali metal cation used increased, the amount of fragmentation decreased. Dorr et al. [31] and Cui et al. [16] observed a similar phenomenon, as discussed in Chapter 1. As the mass of the cation increases, the extent to which the cation is able to move throughout the molecule decreases. For example, the only fragmentation observed for potassium-cationized

samples of levofloxacin and ciprofloxacin is formation of the potassium cation from $[M+K]^+$, yielding no useful structural information. Similarly, potassium cationization of erythromycin only yields neutral loss of cladinose and formation of potassium ion. Also, for all three analyte compounds, sodium cationization yields fewer fragment ions than lithium cationization.

Molecular structure also plays a role in the fragmentation pathways that are observed. For sodium-cationized ciprofloxacin samples, the only observed fragment ion is Na^+. This is also observed for sodium-cationized levofloxacin, but these $[M+Na]^+$ ions also fragment to lose both CO_2 and hydrogen fluoride. Levofloxacin has an additional cyclic structure that ciprofloxacin lacks, but the reasons why this influences the fragmentation behavior remains unclear. Also, both potassium-cationized fluoroquinolones fragment to lose potassium. Potassium-cationized erythromycin samples behave similarly, but potassium is lost at a higher collision voltage and fragmentation of the analyte molecule itself is observed. Because erythromycin has a greater mass than the fluoroquinolones, it has a stronger interaction with potassium.

Alkali metals interact with neutral analytes differently than a proton. A proton has a smaller mass, so it can more readily migrate across the analyte molecule. Because alkali metal cations have masses greater than protons, they are less mobile than protons. Some fragmentation pathways that are unique to protonated analytes may involve migration of the attached proton, and yield ions that cannot be formed form metal cationized analytes. Through blocking of fragmentation pathways that require migration of the proton, alkali metal cationization provides a method to direct fragmentation of pharmaceutical compounds into pathways that provide structural information not

available from protonated species. This feature can be applied to MS/MS metabolite analysis in order to aid determination of structures of pharmaceutical metabolites.

Future Work

To further investigate alkali metal cationization of pharmaceuticals, similar experiments should be conducted on other fluoroquinolones and other macrolide antibiotics and their metabolites. Examination of other classes of pharmaceutical compounds will be pertinent. In addition, generation of metabolites through *in vitro* incubations with liver microsomes, and subjecting the isolated metabolites to alkali metal cationization CID should aid in the determination of the locations and identities of any metabolic alterations.

Other compounds that are metabolically important should also be investigated. For example, fatty acids and their metabolites can serve as biomarkers for various diseases [43]. Many oxylipin metabolites are regioisomers, and alkali metal cationization could provide a means for distinguishing these compounds. LC-MS can also be applied to separate the various regioisomers [44], and post-column addition of alkali metal salts could be used to generate metal cationized ions for subsequent CID analyses.

APPENDIX I

Pseudo-MS^3 spectra for Chapter 2

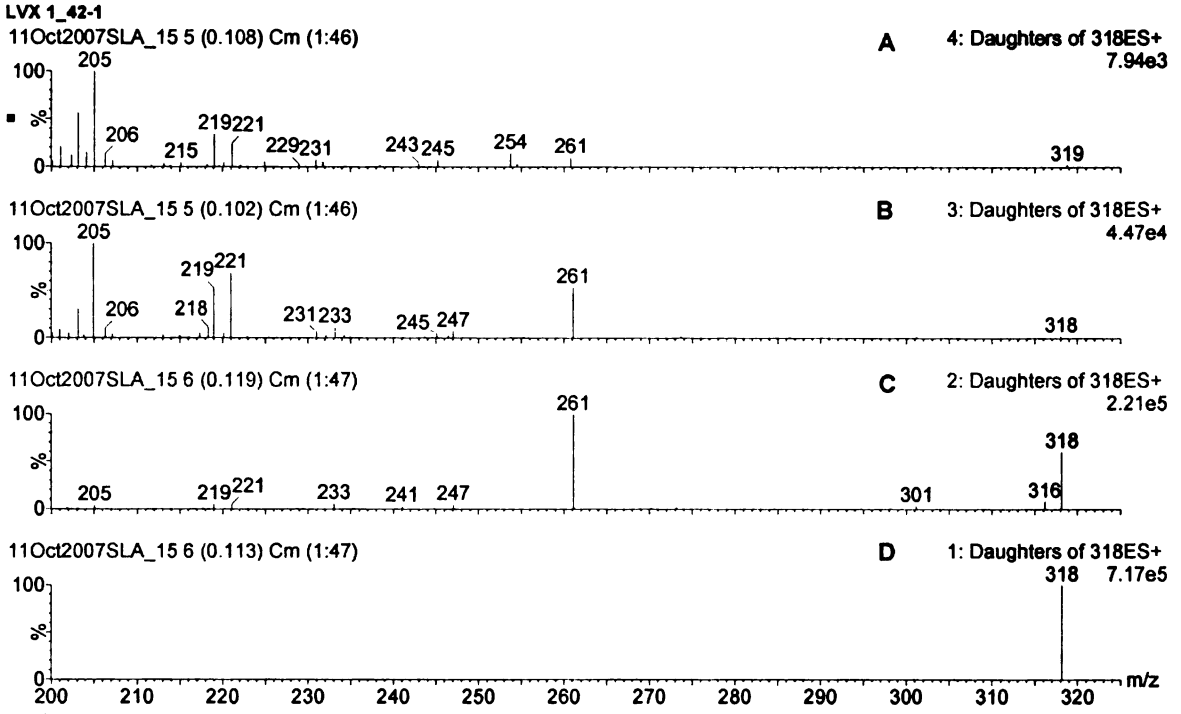

Figure 43. CID product ion spectra of m/z 318 for protonated levofloxacin at (A) 55V, (B) 40 V, (C) 25 V, and (D) 10 V

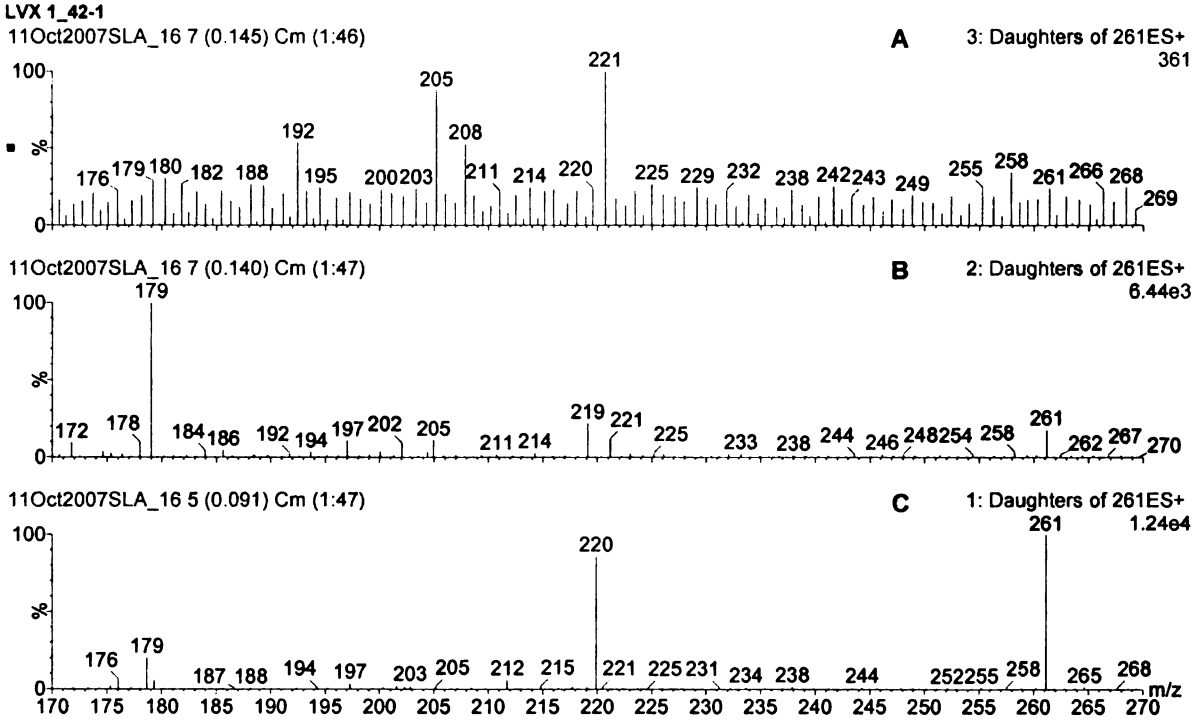

Figure 44. CID product ion spectra of m/z 261 for protonated levofloxacin at (A) 40 V, (B) 25 V, and (C) 10 V

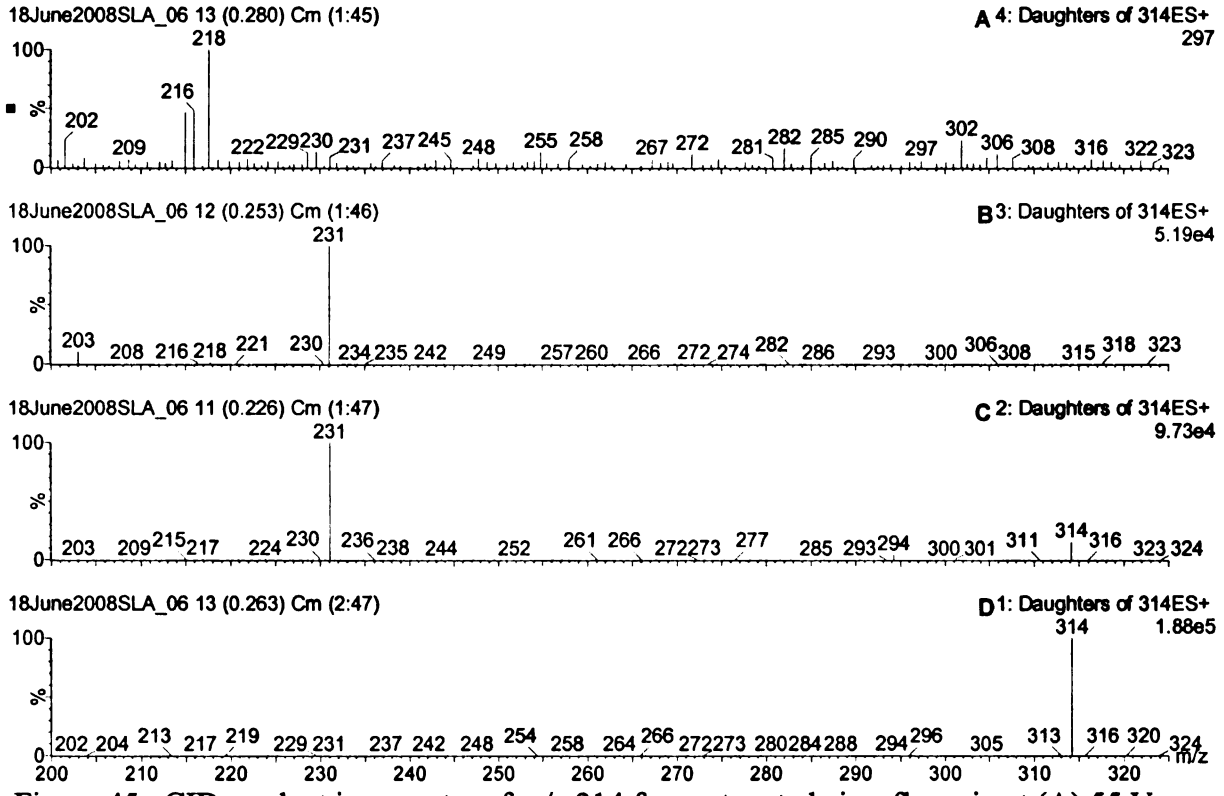

Figure 45. CID product ion spectra of m/z 314 for protonated ciprofloxacin at (A) 55 V, (B) 40 V, (C) 25 V, and (D) 10 V

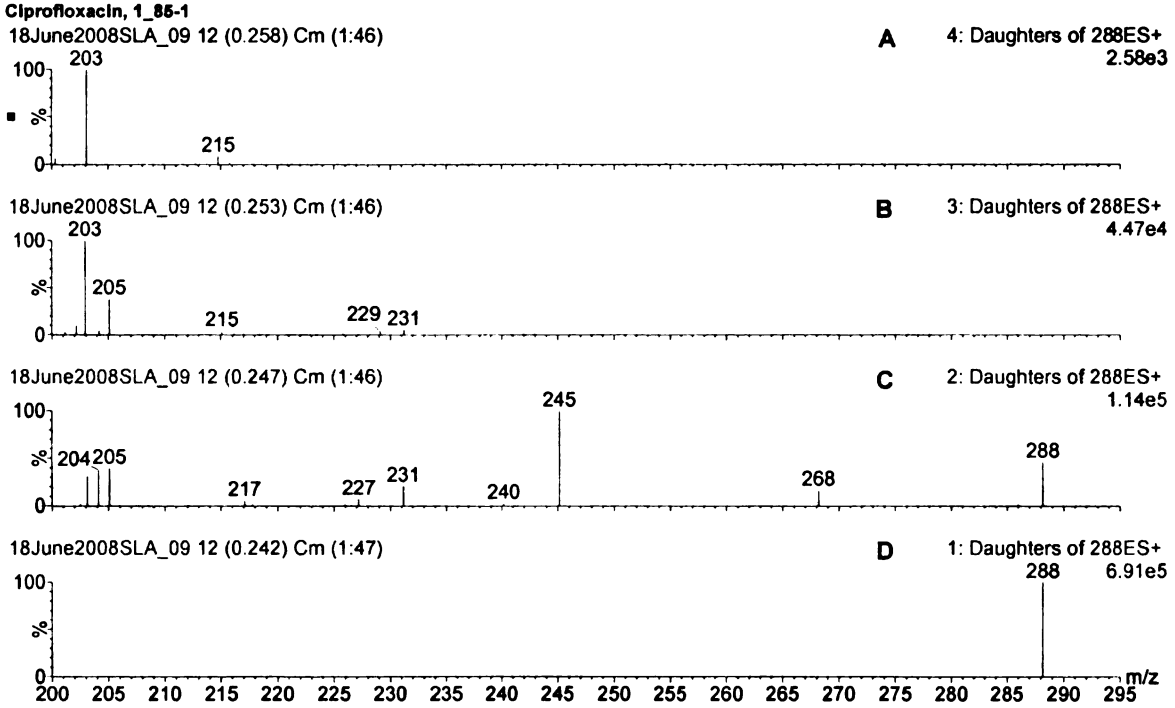

Figure 46. CID product ion spectra of m/z 288 for protonated ciprofloxacin at (A) 55 V, (B) 40 V, (C) 25 V, and (D) 10 V

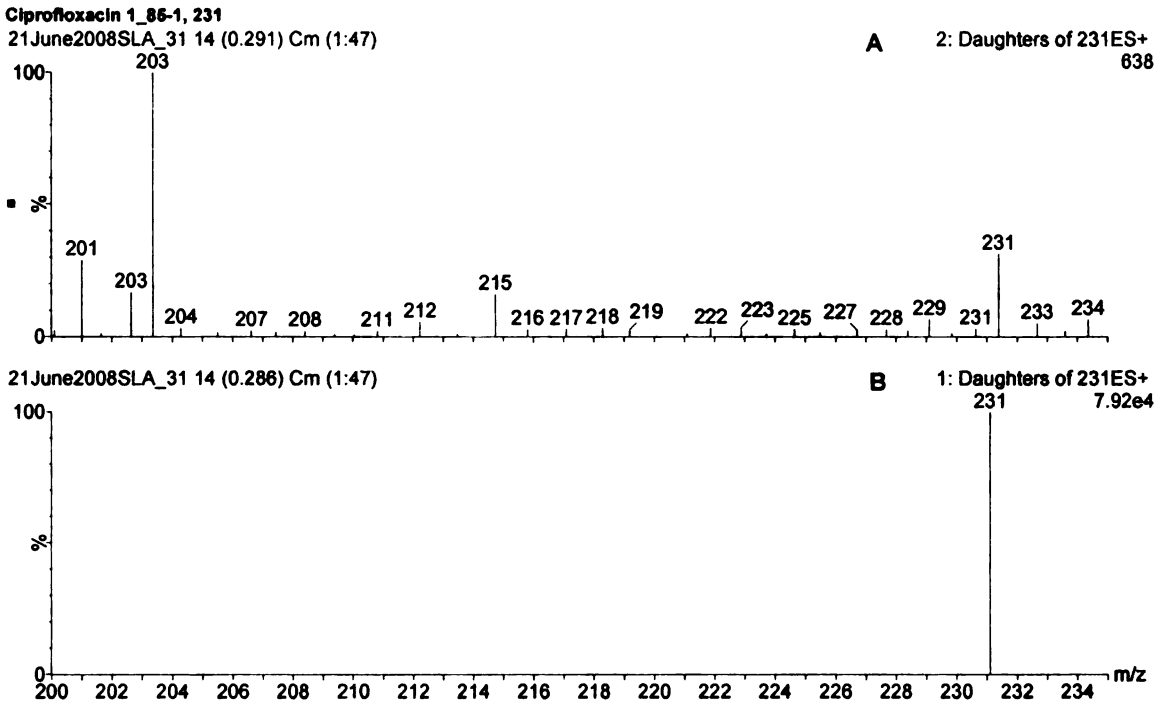

Figure 47. CID product ion spectra of m/z 231 for protonated ciprofloxacin at (A) 25 V and (B) 10 V

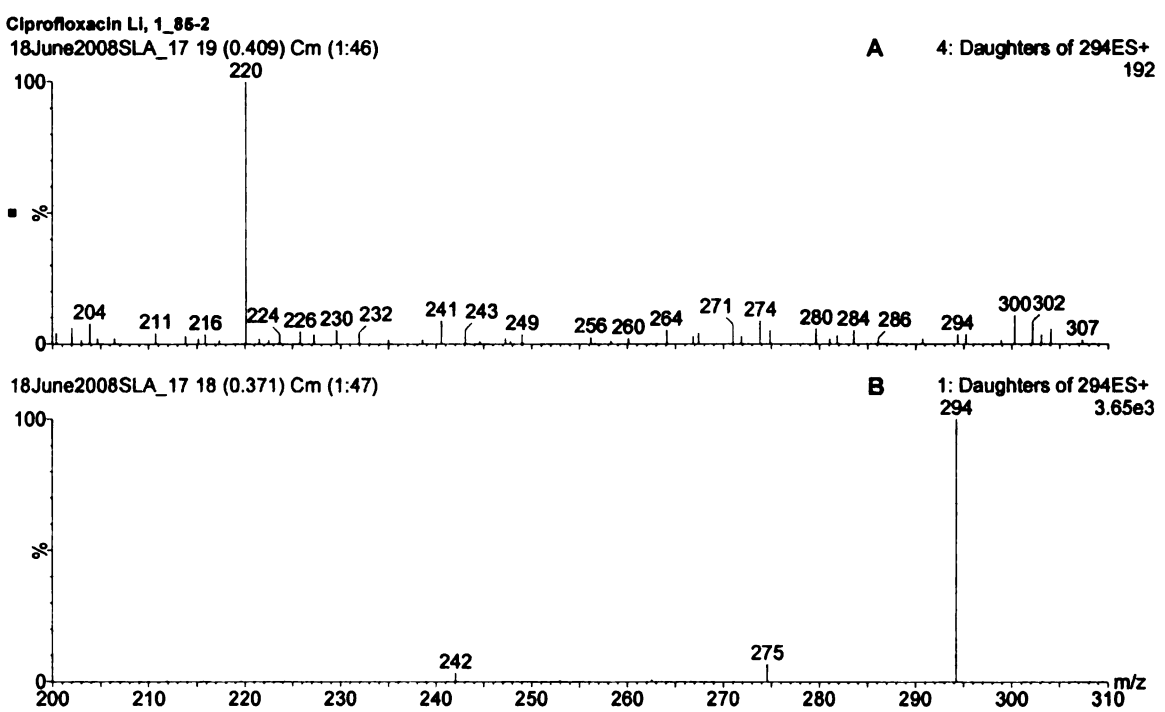

Figure 48. CID product ion spectra of m/z 294 for lithium-cationized ciprofloxacin at (A) 35 V and (B) 10 V

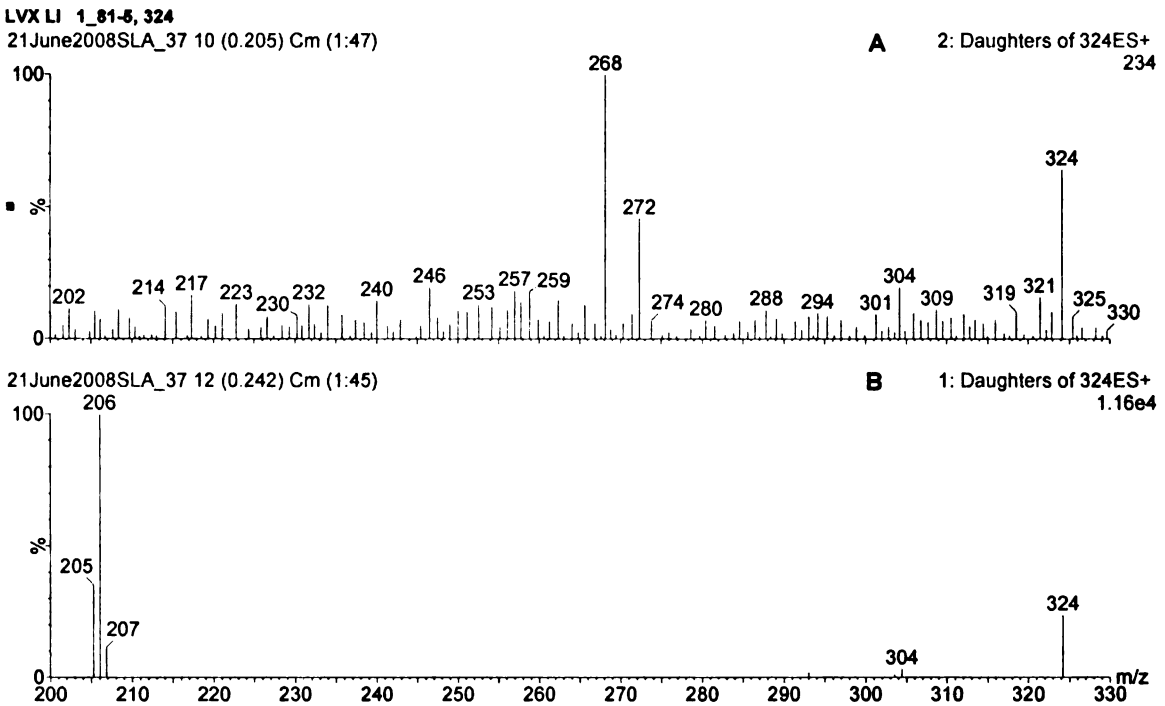

Figure 49. CID product ion spectra of m/z 324 for lithium-cationized levofloxacin at (A) 25 V and (B) 10 V

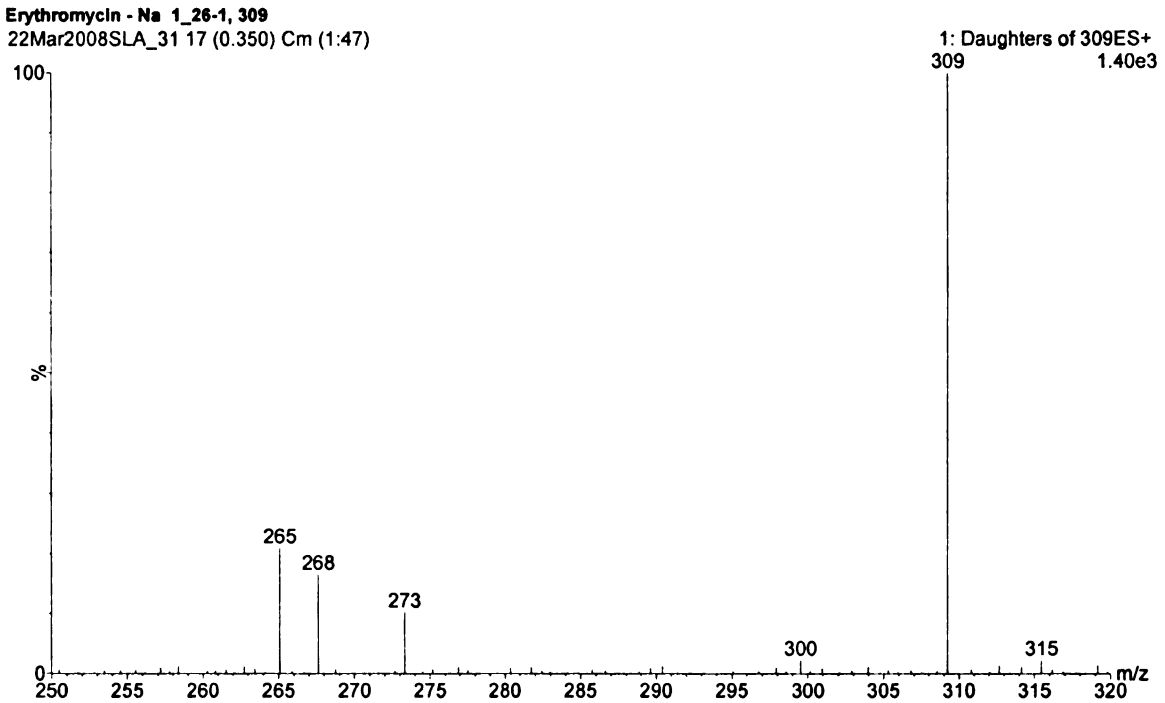

Figure 50. CID product ion spectrum of m/z 309 for sodium-cationized erythromycin at 10 V

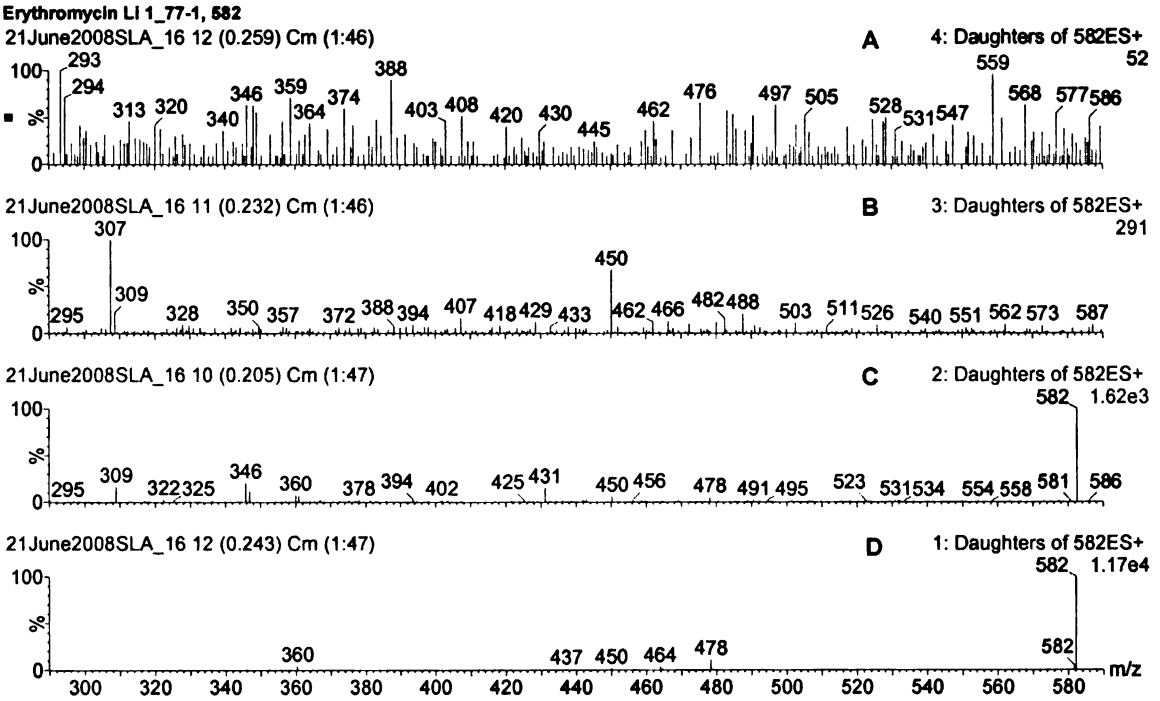

Figure 51. CID product ion spectra of m/z 582 for lithium-cationized erythromycin at (A) 55 V, (B) 40 V, (C) 25 V, and (D) 10 V

APPENDIX II

Tables of Relative Abundances for Mass Spectra in Chapter 2

Table 1. Relative ion abundances for product ion spectra of alkali metal-cationized erythromycin; average values obtained from three sample replicates (values obtained using Waters MassLynx software)

Compound	Parent Ion (m/z)	Fragment Ion (m/z)	% Abundance (10 V)	% Abundance (25 V)	% Abundance (40 V)	% Abundance (55 V)
Erythromycin	734	576	2.4	13.76	0.2	0
		558	0.6	3.75	0.04	0
		540	0.14	2.74	0.03	0
		522	0.17	4.08	0.03	0
		158	0.44	43.61	33.19	11.58
Erythromycin (H/D)	739	580	2.07	11.58	0	0
		561	0.23	1.76	0	0
		542	0	1.03	0	0
		523	0.04	0.69	0	0
		159	0.17	23.24	21.63	6.7

Table 2. Relative ion abundances for product ion spectra of alkali metal-cationized erythromycin; average values obtained from three sample replicates (values obtained using Waters MassLynx software)

Compound	Parent Ion (m/z)	Fragment Ion (m/z)	% Abundance (10 V)	% Abundance (25 V)	% Abundance (40 V)	% Abundance (55 V)
Erythromycin - Na	756	598	0	0.27	24.46	13.33
		423	0	0	0.44	7.81
		309	0	0	0.98	7.21
Erythromycin - Na (H/D)	761	602	0	0	3.69	3.94
		425	0	0	0.45	3.42
		311	0	0.11	0.62	1.75
Erythromycin - Li	740	582	0	0	20.77	0
		564	0	0	8.95	0.79
		520	0	0.01	0.16	0
		468	0	0	1.16	0.27
		407	0	0	2.41	1
		293	0	0	0.91	7.8
Erythromycin - Li (H/D)	745	586	0	0	6.06	0
		567	0	0	2.09	0
		523	0	0.4	0	0.15
		471	0	0	0.29	0.57
		410	0	0	0.37	0.77
		295	0	0	0.53	1.15
Erythromycin - K	772	614	0	0	1.48	0
		39	0	0.24	24.45	30.27

Table 3. Relative ion abundances for protonated levofloxacin; average values obtained from three sample replicates (values obtained using Waters MassLynx software)

Compound	Parent Ion (m/z)	Fragment Ion (m/z)	% Abundance (10 V)	% Abundance (25 V)	% Abundance (40 V)	% Abundance (55 V)
Levofloxacin	362	344	0.11	2.41	0.05	0
		318	4.04	24.41	0.08	0
		261	0.19	36.97	6.95	0.16
		221	0	1.19	5.99	0.94
		205	0	0.66	7.96	4.04
		193	0	0.16	3.1	1.72
Levofloxacin (H/D)	364	344	0	1	0	0
		320	3.84	28.42	0.02	0
		263	0.07	37.76	9.61	0.07
		223	0	0.43	5.46	0.68
		207	0	0.24	4.57	1.81
		195	0	0.05	2.68	2.41

Table 4. Relative ion abundances for alkali metal-cationized levofloxacin; average values obtained from three sample replicates (values obtained using Waters MassLynx software)

Compound	Parent Ion (m/z)	Fragment Ion (m/z)	% Abundance (10 V)	% Abundance (25 V)	% Abundance (30 V)	% Abundance (35 V)
Levofloxacin - Li	368	324	0	13.24	17.78	6.35
		304	0.03	7.3	7.04	1.78
		270	0	2.05	8.81	5.97
Levofloxacin - Li (H/D)	369	325	0.29	7.18	9.12	5.26
		304	0	3.11	1.67	0
		271	1.26	3.63	5.1	3.33
Levofloxacin - Na	384	320	0	2.16	5.81	2.92
		23	0	1.38	2.99	7.01
Levofloxacin - Na (H/D)	385	320	0	1.63	0.51	0.17
		23	0	0.09	2.34	0

Table 5. Relative ion abundances for protonated ciprofloxacin; average values obtained from three sample replicates (values obtained using Waters MassLynx software)

Compound	Parent Ion (m/z)	Fragment Ion (m/z)	% Abundance (10 V)	% Abundance (25 V)	% Abundance (40 V)	% Abundance (55 V)
Ciprofloxacin	332	314	1.57	14.76	0.16	0
		288	3.93	8.01	0	0
		268	0.02	3.56	0	0
		245	0.12	20.09	0.85	0
		231	0.01	7.3	14.75	2.69
		205	0	5.4	4.65	0.34
		203	0	4.06	11.9	4.36
Ciprofloxacin (H/D)	335	315	0.43	8.79	0.06	0
		291	3.49	12.43	0	0
		271	0.03	3.88	0	0
		247	0.02	15.77	0.51	0
		232	0	1.65	9.87	1.42
		207	0	3.86	2.98	0.18
		204	0	0.76	1.98	1.03

Table 6. Relative ion abundances for lithium-cationized ciprofloxacin; average values obtained from three sample replicates (values obtained using Waters MassLynx software)

Compound	Parent Ion (m/z)	Fragment Ion (m/z)	% Abundance (10 V)	% Abundance (25 V)	% Abundance (30 V)	% Abundance (35 V)
Ciprofloxacin - Li	338	294	0.14	22.16	14.65	5.65
		274	0	0.29	0.68	0.46
		211	0	0.79	3.41	9.48
Ciprofloxacin - Li (H/D)	340	296	0.03	25.62	26.47	2.48
		275	0	0.44	2.1	4
		213	0.01	0.36	1.74	5.87

BIBLIOGRAPHY

BIBLIOGRAPHY

1. Tolonen, A., et al., *A simple method for differentiation of monoisotopic drug metabolites with hydrogen-deuterium exchange liquid chromatography/electrospray mass spectrometry.* European Journal of Pharmaceutical Sciences, 2005. **25**(1): p. 155-162.

2. Kanazawa, H., et al., *Determination of omeprazole and its metabolites in human plasma by liquid chromatography-mass spectrometry.* Journal of Chromatography A, 2002. **949**(1-2): p. 1-9.

3. Bauer, K.S., S.C. Dixon, and W.D. Figg, *Inhibition of angiogenesis by thalidomide requires metabolic activation, which is species-dependent.* Biochemical Pharmacology, 1998. **55**(11): p. 1827-1834.

4. Hatfill, S.J., et al., *Induction of Morphological-Differentiation in the Human Leukemic-Cell Line K562 by Exposure to Thalidomide Metabolites.* Leukemia Research, 1991. **15**(2-3): p. 129-136.

5. Purnapatre, K., S.K. Khattar, and K.S. Sain, *Cytochrome P450s in the development of target-based anticancer drugs.* Cancer Letters, 2008. **259**(1): p. 1-15.

6. Dalla Corte, C.L., Fachinetto, R., Colle, D., Pereira, R.P., Avila, D.S., Villarinho, J.G., Wagner, C., Pereira, M.E., Nogueira, C.W., Soares, F.A.A., Rocha, J.B.T. , *Potentially adverse interactions between haloperidol and valerian.* Food and Chemical Toxicology, 2008. **46**: p. 2369-2375.

7. Hellum, B.H., Z.H. Hu, and O.G. Nilsen, *The induction of CYP1A2, CYP2D6 and CYP3A4 by six trade herbal products in cultured primary human hepatocytes.* Basic & Clinical Pharmacology & Toxicology, 2007. **100**(1): p. 23-30.

8. Umathe, S.N., et al., *Quercetin pretreatment increases the bioavailability of pioglitazone in rats: Involvement of CYP3A inhibition.* Biochemical Pharmacology, 2008. **75**(8): p. 1670-1676.

9. Siuzdak, G., *Mass Spectrometry for Biotechnology.* 1996, San Diego: Academic Press.

10. de Hoffmann, E., Stroobant, V, *Mass Spectrometry: Principles and Applications* 3rd ed. 2007, West Sussex: John Wiley & Sons Ltd.

11. Kebarle, P. and L. Tang, *From Ions in Solution to Ions in the Gas-Phase - the Mechanism of Electrospray Mass-Spectrometry.* Analytical Chemistry, 1993. **65**(22): p. A972-A986.

12. Gates, P. *Electrospray Ionisation (ESI).* 2004 Jan. 20, 2004 [cited 2008 May 23, 2008]; Available from: http://www.chm.bris.ac.uk/ms/theory/esi-ionisation.html.

13. Gabelica, V., De Pauw, E., *Internal energy and fragmentation of ions produced in electrospray sources.* Mass Spectrom Rev, 2005. **24**: p. 566-587.

14. Yost, R.A. and C.G. Enke, *Triple Quadrupole Mass-Spectrometry for Direct Mixture Analysis and Structure Elucidation.* Analytical Chemistry, 1979. **51**(12): p. 1251-&.

15. Sleno, L., Volmer D.A., *Ion activation methods for tandem mass spectrometry.* J. Mass Spectrom., 2004. **39**: p. 1091-1112.

16. Cui, M., Song, F., Liu, Z., Liu, S., *Metal ion adducts in the structural analytsis of ginsenosides by electrospray ionization with multi-stage mass spectrometry.* Rapid Commun. Mass Spectrom., 2001. **15**: p. 586-595.

17. Madhusudanan, K.P., Raj, K., Bhaduri, A.P. , *Effect of metal cationization on the low-energy collision-induced dissociation of loganin, epi-loganin and ketoganin studied by electrospray ionization tandem mass spectrometry.* J. Mass Spectrom., 2000. **35**: p. 901-911.

18. Adams, J. and M.J. Songer, *Charge-Remote Fragmentations for Structural Determination of Lipids.* Trac-Trends in Analytical Chemistry, 1993. **12**(1): p. 28-36.

19. Cheng, C.F. and M.L. Gross, *Applications and mechanisms of charge-remote fragmentation.* Mass Spectrometry Reviews, 2000. **19**(6): p. 398-420.

20. Lopes, N.P., et al., *Fragmentation studies on monensin A and B by accurate-mass electrospray tandem mass spectrometry.* Rapid Communications in Mass Spectrometry, 2002. **16**(5): p. 414-420.

21. Lopes, N.P., et al., *Fragmentation studies on monensin A by sequential electrospray mass spectrometry.* Analyst, 2002. **127**(4): p. 503-506.

22. Lopes, N.P., Almeida-Paz, F.A., and Gates, P.J., *Influence of the alkali metal cation on the fragmentation of monensin in ESI-MS/MS.* Brazilian Journal of Pharmaceutical Sciences, 2006. **42**(3): p. 363-367.

23. Smith, G. and J.A. Leary, *Mechanistic studies of diastereomeric nickel(II) N-glycoside complexes using tandem mass spectrometry.* Journal of the American Chemical Society, 1998. **120**(50): p. 13046-13056.

24. Ann, Q.H. and J. Adams, *Collision-Induced Decomposition of Sphingomyelins for Structural Elucidation.* Biological Mass Spectrometry, 1993. **22**(5): p. 285-294.

25. Ann, Q.H. and J. Adams, *Structure-Specific Collision-Induced Fragmentations of Ceramides Cationized with Alkali-Metal Ions.* Analytical Chemistry, 1993. **65**(1): p. 7-13.

26. Ann, Q. and J. Adams, *Structure Determination of Ceramides and Neutral Glycosphingolipids by Collisional Activation of [M + Li]+ Ions.* Journal of the American Society for Mass Spectrometry, 1992. **3**(3): p. 260-263.

27. Adams, J. and M.L. Gross, *Tandem Mass-Spectrometry for Collisional Activation of Alkali-Metal-Cationized Fatty-Acids - a Method for Determining Double-Bond Location.* Analytical Chemistry, 1987. **59**(11): p. 1576-1582.

28. Asam, M.R. and G.L. Glish, *Tandem mass spectrometry of alkali cationized polysaccharides in a quadrupole ion trap.* Journal of the American Society for Mass Spectrometry, 1997. **8**(9): p. 987-995.

29. Madhusudanan, K.P., Raj, K., Bhaduri, A.P., *Effect of alkali metal cationization and multiple alkali metal exchange on the collision-induced dissociation of loganic acid studied by electrospray ionization tandem mass spectrometry.* Rapid Commun. Mass Spectrom., 2000. **14**: p. 885-896.

30. Adams, J. and M.L. Gross, *Energy-Requirements for Remote Charge Site Ion Decompositions and Structural Information from Collisional Activation of Alkali-Metal Cationized Fatty Alcohols.* Journal of the American Chemical Society, 1986. **108**(22): p. 6915-6921.

31. Dorr, F.A., Tomaz, J.C., Lopes, N.P., and Pinto, E., *Comparitive analysis of the gas-phase reactions of cylindrospermopsin and the difference in the alkali metal cation mobility.* Rapid Commun. Mass Spectrom., 2008. **22**: p. 2015-2020.

32. Sprandel, K.A., Bodvold, K.A., *Safety and Tolerability of Fluoroquinolones.* Clinical Cornerstone, 2003. **Supplement 3**: p. S29-S36.

33. Sarkar, M., et al., *Invitro Effect of Fluoroquinolones on Theophylline Metabolism in Human Liver-Microsomes.* Antimicrobial Agents and Chemotherapy, 1990. **34**(4): p. 594-599.

34. Derby, L.E., et al., *Erythromycin-Associated Cholestatic Hepatitis.* Medical Journal of Australia, 1993. **158**(9): p. 600-602.

35. Karthik, S.V. and D. Casson, *Erythromycin associated cholestatic hepatitis and liver dysfunction in children: The British experience.* Journal of Clinical Gastroenterology, 2005. **39**(8): p. 743-744.

36. Lindstrom, T.D., B.R. Hanssen, and S.A. Wrighton, *Cytochrome-P-450 Complex-Formation by Dirithromycin and Other Macrolides in Rat and Human Livers.* Antimicrobial Agents and Chemotherapy, 1993. **37**(2): p. 265-269.

37. Zweers-Zeilmaker, W.M., et al., *In vitro complex formation and inhibition of hepatic cytochrome P450 activity by different macrolides and tiamulin in goats and cattle.* Research in Veterinary Science, 1999. **66**(1): p. 51-55.

38. D'Agostino, P.A., J.R. Hancock, and L.R. Provost, *Electrospray Mass-Spectrometric Characterization of Fluoroquinolone Antibiotics - Norfloxacin, Enoxacin, Ciprofloxacin and Ofloxacin.* Rapid Communications in Mass Spectrometry, 1995. **9**(11): p. 1038-1043.

39. Hemeryck, A., et al., *Pharmacokinetics, metabolism, excretion, and plasma protein binding of 14C-levofloxacin after single oral administration in the Rhesus monkey.* Drug Metabolism Reviews, 2005. **37**: p. 43-43.

40. Crowe, M.C., et al., *Characterization of erythromycin analogs by collisional activated dissociation and infrared multiphoton dissociation in a quadrupole ion trap.* Journal of the American Society for Mass Spectrometry, 2002. **13**(6): p. 630-649.

41. Gates, P.J., et al., *Structural elucidation studies of erythromycins by electrospray tandem mass spectrometry.* Rapid Communications in Mass Spectrometry, 1999. **13**(4): p. 242-246.

42. Kearney, G.C., et al., *Structural elucidation studies of erythromycins by electrospray tandem mass spectrometry II.* Rapid Communications in Mass Spectrometry, 1999. **13**(16): p. 1650-1656.

43. Waugh, R.J., et al., *Identification and relative quantitation of F-2-isoprostane regioisomers formed in vivo in the rat.* Free Radical Biology and Medicine, 1997. **23**(6): p. 943-954.

44. Orellana-Coca, C., et al., *Analysis of fatty acid epoxidation by high performance liquid chromatography coupled with evaporative light scattering detection and mass spectrometry.* Chemistry and Physics of Lipids, 2005. **135**(2): p. 189-199.